INORGANIC CHEMISTRY
FRONTIERS

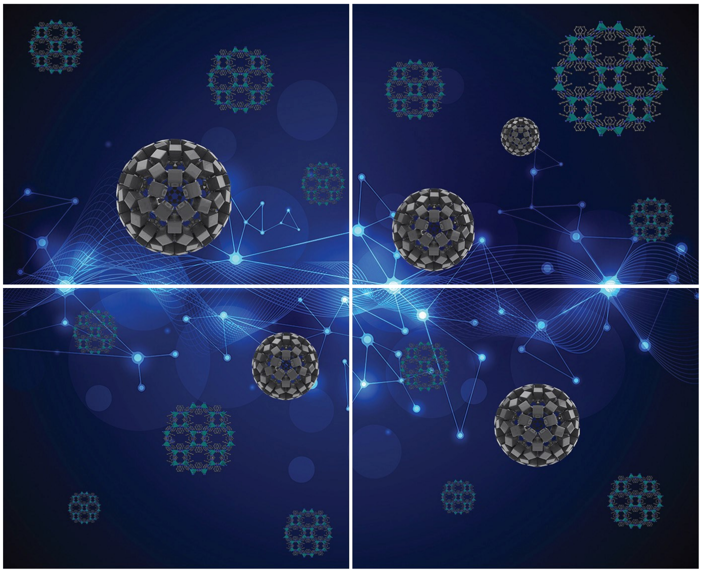

This article can be cited before page numbers have been issued, to do this please use: R. L. Lin, J. Liu, K. Chen and C. Redshaw, *Inorg. Chem. Front.*, 2020, DOI: 10.1039/D0QI00529K.

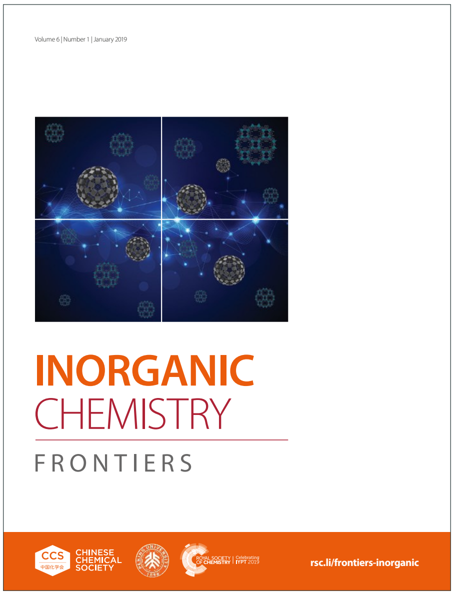

Supramolecular Chemistry of Substituted Cucurbit[*n*]urils

View Article Online
DOI: 10.1039/D0QI00529K

Rui-Lian Lin, [a] *Jing-Xin Liu,* [a,] * *Kai Chen* [b,] * *and Carl Redshaw* [c]

---

[a] College of Chemistry and Chemical Engineering, Anhui University of Technology, Maanshan 243002, P. R. China. jxliu411@ahut.edu.cn

[b] Collaborative Innovation Center of Atmospheric Environment and Equipment Technology, Jiangsu Key Laboratory of Atmospheric Environment Monitoring and Pollution Control, School of Environmental Science and Engineering, Nanjing University of Information Science & Technology, Nanjing 210044, P. R. China. Email: catqchen@163.com or kaichen85@nuist.edu.cn

[c] Department of Chemistry & Biochemistry, University of Hull, Hull HU6 7RX, UK

Abstract

Since the first example of substituted cucurbit[*n*]urils (Q[*n*]), decamethylcucurbit[5]uril ($Me_{10}Q[5]$), was reported in 1992, numerous substituted Q[*n*]s have been synthesized and studied. In this review article, we focuses on the recognition properties of the substituted Q[*n*]s toward a variety of organic species as well as the coordination chemistry of substituted Q[*n*]s with different metal ions, including alkali/alkaline-earth metals, transition metals, and lanthanides. Applications of substituted Q[*n*]s, and the self-assembly processes affording mechanically interlocked molecules (MIMs) are also described. The main purpose of this review is to highlight important advances in the blossoming field of substituted Q[*n*]s, which will likely be of interest to researchers in supramolecular chemistry.

Keywords: Coordination chemistry; Mechanically interlocked molecules; Molecular recognition; Substituted cucurbit[*n*]urils; Supramolecular chemistry.

Contents

View Article Online
DOI: 10.1039/D0QI00529K

View Article Online
DOI: 10.1039/D0QI00529K

View Article Online
DOI: 10.1039/D0QI00529K

1. Introduction

Since the first macrocyclic polyether, dibenzo[18]crown-6, was reported by Pedersen back in 1967[1,2], host−guest/supramolecular chemistry has experienced rapid development. Host−guest/supramolecular chemistry usually involves the molecular recognition and inclusion of substrates by macrocyclic compounds, such as cyclodextrins (α, β and γ), calix[*n*]arenes, pillar[*n*]arenes, and various cyclophanes.[3–9] Cucurbit[*n*]uril (*n* = 5-8, 10, 13-15, commonly abbreviated as Q[*n*]s or CB[*n*]s, Figure 1)[5,10–20], a family of artificial macrocyclic hosts, have in recent years played a central role in supramolecular chemistry, which reflects their excellent properties in molecular recognition and molecular assembly. The journey for Q[*n*]s started in 1905, when a white solid (Q[6]), was prepared by Behrend and co-workers, although its composition and structure was not known at that time.[21] Seventy-five years later, Freeman *et al.* restudied the synthesis of the white solid and ascertained the structure of Q[6] via the use of X-ray diffraction.[22] Since then, Q[6] has been used for studied for both metal ion coordination and small molecule inclusion. After the discovery of a series of Q[*n*] homologues in 2000 and 2001 by Kim and Day,[23,24] research activity in Q[*n*] chemistry progressed greatly, and has impacted on a wide range of fields, including sensing, catalysis, drug delivery, nano-materials and stimuli-responsive systems.

The common Q[*n*] homologues comprise *n* glycoluril units linked by 2*n* methylene (Figure 1). They feature a hydrophobic cavity with different sizes, two polar carbonyl portals with negative electrostatic potential, and a circular outer surface with positive electrostatic potential. Based on these structural features, Q[*n*]s can accommodate hydrophobic molecules or groups of suitable size in their cavities, coordinate to various metal ions at their portals, and connect with electronegative species through their outer surfaces. As a result, many research groups have reported a large number of Q[*n*] complexes with different metal ions, anions and charged

View Article Online
DOI: 10.1039/D0QI00529K

organic molecules.[5,10–20] Although Q[*n*] homologues are outstanding macrocyclic hosts for fundamental and applied molecular recognition, three main shortcomings still hinder their researches and applications. Firstly, Q[*n*] homologues have poor solubility in pure water and in most common organic solvents, especially the Q[6], Q[8], and Q[10] systems. Most host−guest chemistry research on Q[*n*] homologues has to be performed in acid solution or in the presence of alkali metal ion, which strongly affects the binding affinity between the host and the guest, as illustrated by Buschmann,[25] Kaifer,[26] Nau,[27] and Kim[28] *et al*. Secondly, although the sizes and shapes of the guests are diverse, Q[*n*] homologues (except for Q[13-15]) possess high symmetrical cavities. Consequently, Q[*n*] homologues fail to selectively recognize some guest molecules with special shape.[75-77, 142, 152] Thirdly, in comparison with other macrocyclic hosts, for example the calix[*n*]arenes, Q[*n*] homologues are difficult to functionalize. To overcome these shortcomings, significant efforts have been invested on the design and synthesis of substituted Q[*n*]s.

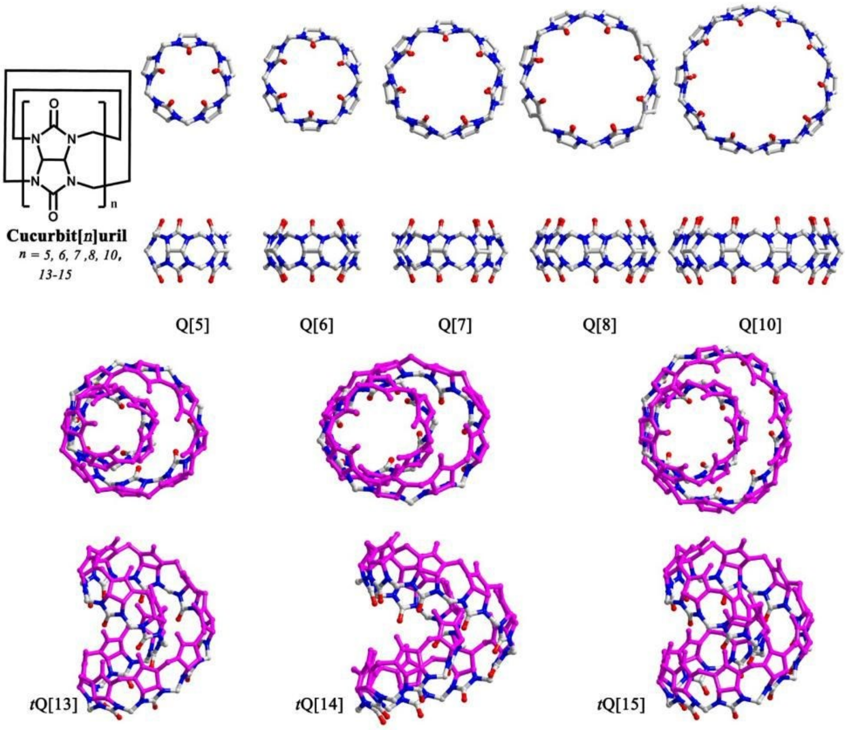

Figure 1. X-ray crystal structures of cucurbit[*n* = 5-8, 10, 13-15]urils.

View Article Online
DOI: 10.1039/D0QI00529K

Over the past two decades or so, various substituted Q[*n*]s have been prepared.[29–60] As will be discussed later, the host−guest/supramolecular properties exhibited by substituted Q[*n*]s reveal advantages *versus* Q[*n*]s. 1) Substitutions greatly increase solubility of substituted Q[*n*]s by decreasing solid-state packing. 2) Unsymmetrical substitutions deform the cavity symmetry and open up better selectivity to guest sequestration.[39,40,50,56] It should be noted that Q[*n*]s are amongst some of the most selective hosts because of their different cavity sizes. 3) Substitutions greatly increase the functionalizability of Q[*n*] homologues. 4) By creating substituted Q[*n*]s and increasing the diversification of the structures, more complex chemical systems such as complicated molecular machines and smart sensors can be built.

Although great progress has been achieved in Q[*n*]s chemistry and numerous reviews have appeared,[10–20] few focus on the field of substituted Q[*n*]s. This review article will highlight advances in field of substituted Q[*n*]s. We will begin by discussing the synthesis of classical substituted Q[*n*]s, such as fully and partially methyl-substituted Q[*n*]s, cyclohexano-substituted Q[*n*]s, cyclopentano-substituted Q[*n*]s, hydroxy-substituted Q[*n*]s, and substituted Q[*n*]s with mixed substitutions. We will then focus on the host−guest complexation properties of the substituted Q[*n*]s, their inclusion and coordination compounds, plus mechanically interlocked molecules (MIMs) and molecular devices, including many examples from our own group's efforts.

2. Synthesis of substituted Q[*n*]s

Back in 1992, Stoddart and co-workers reported the first example of a substituted Q[*n*], namely decamethylcucurbit[5]uril ($Me_{10}Q[5]$).[29] The reaction of 2,3-butanedione with urea under acidic conditions leads to dimethylglycoluril. Condensation of dimethylglycoluril with formaldehyde in acidic medium generates a white precipitate of $Me_{10}Q[5]$ (Table 1). Since then,

DOI: 10.1039/D0QI00529K

a variety of Q[*n*] derivatives, including fully and partially alkyl-substituted Q[*n*], hemicucurbit[*n*]uril,[30,31] biotin[6]uril,[32] bambus[6]uril,[33] and acyclic Q[*n*] congeners,[34,35] have been synthesized by Day, Isaacs, Kim, Sindelar, Tao and other groups. Note that the present review focuses on substituted Q[*n*]s, those Q[*n*] derivatives where the basic skeleton is preserved, as shown in Table 1.

In 2001, Kim *et al.* synthesized fully substituted cyclohexanoQ[*n*]s (abbreviated as $CyH_nQ[n]$s, $n = 5, 6$), which are soluble not only in water but also in some organic solvents.[36] Day and coworkers synthesized two other kinds of fully substituted Q[*n*], the cyclopentanoQ[*n*][37] (abbreviated as $CyP_nQ[n]$, $n = 5, 6, 7$) in 2012 and the cyclobutanoQ[*n*][38] (abbreviated as $CyB_nQ[n]$, $n = 5\text{-}8$) in 2017. The syntheses of these fully substituted Q[*n*]s have similar procedures: the synthesis of the substituted glycoluril (precursor), and condensation of substituted glycoluril with formaldehyde in acidic medium.

Tao group prepared the first example of a partially methyl-substituted Q[*n*], the symmetrical tetramethylcucurbit[6]uril (TMeQ[6]) in 2004.[39] The synthetic procedure involved the diether of dimethylglycoluril and the glycoluril dimer. Using similar strategies and appropriate building blocks, Tao group later prepared a series of partially methyl-substituted Q[*n*]s, such as the symmetrical octamethyl-substituted cucurbit[6]uril[40] (OMeQ[6]), *ortho*-tetramethyl-substituted cucurbit[6]uril[41] (*o*-TMeQ[6]), *meta*-tetramethyl-substituted cucurbit[8]uril[42] (*m*-$Me_4Q[8]$). Moreover, the same group has recently synthesized a series of hemimethyl-substituted cucurbit[*n*]urils ($HMe_nQ[n]$s, $n = 5, 6, 7$) using the precursor 3α-Methylglycoluril.[43–45] A series of partially cyclohexano-substituted cucurbit[6]uril such as the *para*-dicyclohexanocucurbit[6]uril[46] ($CyH_2Q[6]$) and *meta*-tricyclohexanocucurbit[6]uril[47] ($CyH_3Q[6]$) and some substituted Q[*n*]s with mixed substituents[48] were isolated. Concomitantly, the toxicity of $HMe_7Q[7]$ was studied by Wang and co-workers, revealing that

View Article Online
DOI: 10.1039/D0QI00529K

$HMe_7Q[7]$ exhibited a good biocompatibility profile.[49] Other groups also reported the synthesis of methyl- and cyclohexano-substituted Q[*n*]. The Isaacs group in 2015 presented a building block strategy for the synthesis of *ortho*-tetramethyl-substituted cucurbit[8]uril (*o*-$Me_4Q[8]$) and *ortho*-dicyclohexano-substituted cucurbit[8]uril (*o*-$CyH_2Q[8]$) by condensation of glycoluril hexamer with bis(cyclic ethers) under well-defined conditions.[50]

One of the shortcomings of the Q[*n*] homologues is that they are difficult to functionalize. To overcome this long-standing problem, Kim *et al.* created an effective procedure in 2003 via the oxidation the Q[*n*] homologues with $K_2S_2O_8$ in water to produce their corresponding hydroxy-substituted $(HO)_mQ[n]$s (n = 5-8, m = 10, 12, 14 and 16), which can then be further modified to afford tailored Q[*n*] derivatives.[51] The Kim group recently demonstrated a superacid-mediated conversion of the hydroxyl group on Q[*n*]s (n = 6 and 7) to yield other important functional groups in high yields.[52] Additionally, they found that the resulting substituted Q[*n*] can be readily conjugated to an enzyme to afford a Q[*n*]-conjugated enzyme which is useful in protein blotting assays.[53]

Other groups also have made significant progress towards functionalizing Q[*n*] homologues. In 2012, Scherman and co-workers prepared monohydroxylated Q[6] through the controlled oxidation of Q[6] in the presence of a tailor-made bisimidazolium guest.[54] In the same year, the Isaacs group presented a building-block approach for mono-functionalization of some substituted Q[7]s.[55] Interestingly, the mono-functionalized Q[7] exhibit self-association into tetrameric aggregates in aqueous solution, as shown in Figure 2. In 2015, the Isaacs group synthesized hydrophobic monofunctionalized Q[7], which can undergo self-inclusion complexation and form vesicle-type assemblies.[56] Ouari and Bardelang *et al.* reported a photochemical method for producing hydroxy-substituted $(HO)_mQ[n]$s using hydrogen peroxide and UV light.[57,58] Very recently, Kaifer, Dong and coworkers obtained monohydroxylated cucurbit[7]uril ($(HO)_1Q[7]$) through the direct oxidation of Q[7].[59]

View Article Online
DOI: 10.1039/D0QI00529K

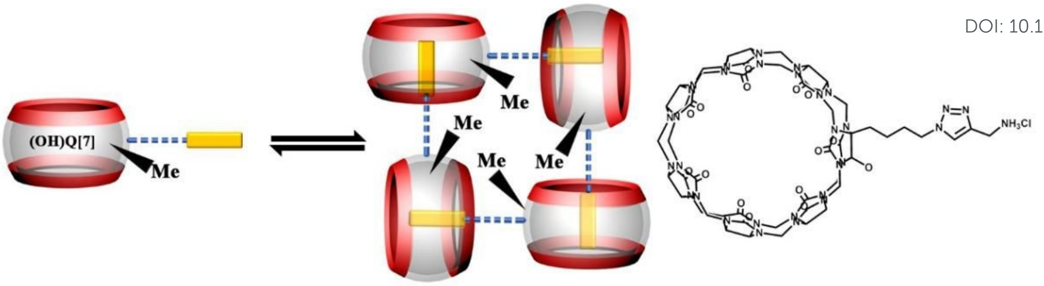

Figure 2. Mono-functionalized Q[7] self-associated into tetrameric aggregates.

By simply mixing glycoluril, paraformaldehyde, and another aldehyde, Sindelar and coworkers prepared a novel type of monosubstituted Q[6], mono(2-phenylethyl)cucurbit[6]uril (PheQ[6]).[60] Different from the above mentioned substituted Q[*n*]s, the substituent is attached to one methylene bridge of the PheQ[6] (Figure 3a and 3b). Impressively, the monosubstituted Q[6] macrocycles self-assembled into tetrameric aggregates (Figure 3c) in the solid state. Compared to the PheQ[6], it is impossible for unsubstituted Q[*n*]s to self-associate into polymers without the assistance of other compounds.

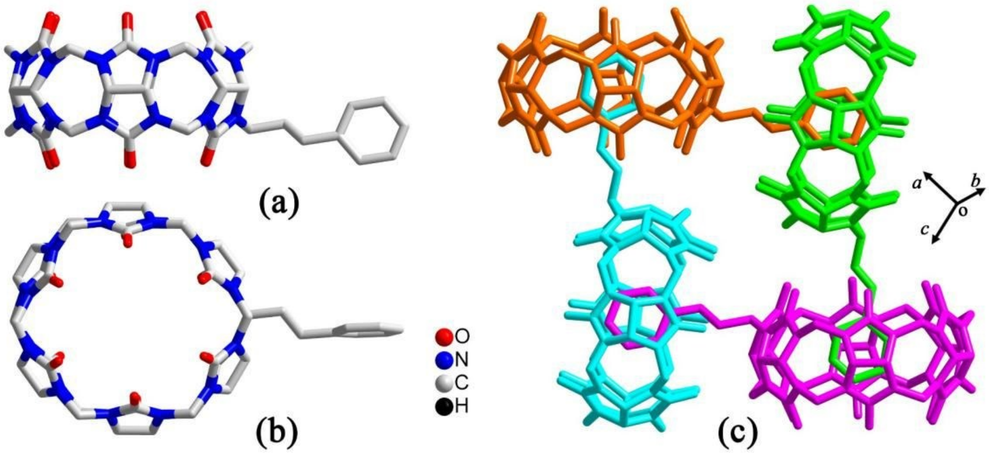

Figure 3. Crystal structures of tetramer based on mono(2-phenylethyl)cucurbit[6]uril (PheQ[6]).

3. Molecular recognition of substituted Q[*n*]s

3.1. Binding behaviour of alkyldiammonium ions toward substituted Q[*n*]s

View Article Online
DOI: 10.1039/D0QI00529K

In their pioneering work, Collet, Cram, Rebek, *et al.* observed that molecular behaviour including conformations and reactivity in small spaces can be quite different from that in dilute solution.[61-64] With this in mind, the molecular behavior of different alkyl chains in the hydrophobic cavities of the Q[*n*] derivatives can also be regarded as another study of a kind of small space. Therefore, the binding interactions between a series of alkyldiammonium ions and a variety of substituted Q[6], including TMeQ[6][65,66], CyH$_2$Q[6][67], CyH$_6$Q[6][67], and CyP$_6$Q[6][68] has been investigated both in aqueous solution and in the solid state. NMR spectra and single-crystal X-ray diffraction analyses revealed that the binding behaviour varies depending upon the alkyl chain length. Here, the TMeQ[6] is taken as a representative example for discussion (Figure 4). 1,2-Ethanediammonium resides outside the portals of the TMeQ[6] and binds *exo* to the host portals forming an exclusion complex. Other longer alkyldiammonium guests can be accommodated in the cavity of the TMeQ[6] forming 1:1 inclusion complexes. Interestingly, if the alkyl chain length is longer than the height of the cavity of the TMeQ[6], then the alkyl chains usually take a contorted conformation. Isothermal titration calorimetry (ITC) experiments indicated that the binding of the alkyldiammonium guests with the substituted Q[6] is mainly enthalpy driven, which benefits from hydrophobic effects and host−guest interactions. It is accepted that the main driving force for the assembly of the inclusion complex based on Q[*n*] is the hydrophobic effect.[69] However, the binding of the charged alkyldiammonium guests with the substituted Q[6] should also take into account the host−guest interactions, including ion−dipole interactions and van der Waals interactions.

View Article Online
DOI: 10.1039/D0QI00529K

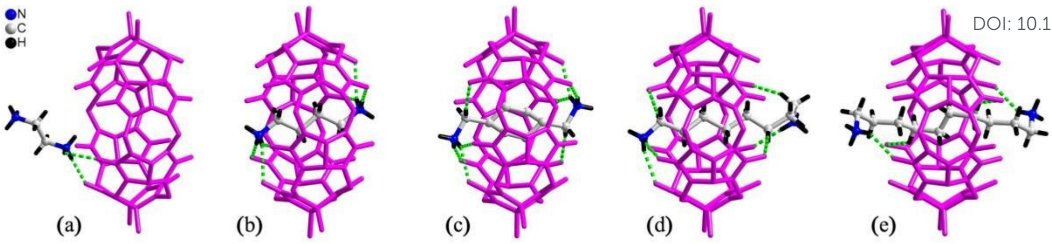

Figure 4. Extended and contorted conformations of alkanediammonium ions in the cavity of TMeQ[6].

$HMe_6Q[6]$ is soluble in water as well as in DMSO. The binding behaviour of $HMe_6Q[6]$ towards alkyldiammonium ions in aqueous solution is completely different from that observed in the organic solvent DMSO.[70] In aqueous solution, the alkyl chains of the alkyldiammonium ions were encapsulated into the $HMe_6Q[6]$ cavity, forming an inclusion complex. In contrast, in DMSO, the $HMe_6Q[6]$ engulfs only the NH_3^+ groups of the alkyldiammonium ions, forming a head-inclusion complex, which can be switched to supramolecular polymers upon heating (Figure 5). Recently, we also compared the binding behaviour of $HMe_7Q[7]$ with alkyldiammonium ions (protonated guests) and their corresponding uncharged and alkyldiamines in aqueous solution.[71] The results suggested that the driving force for the host−guest binding is related to the features of the guests.

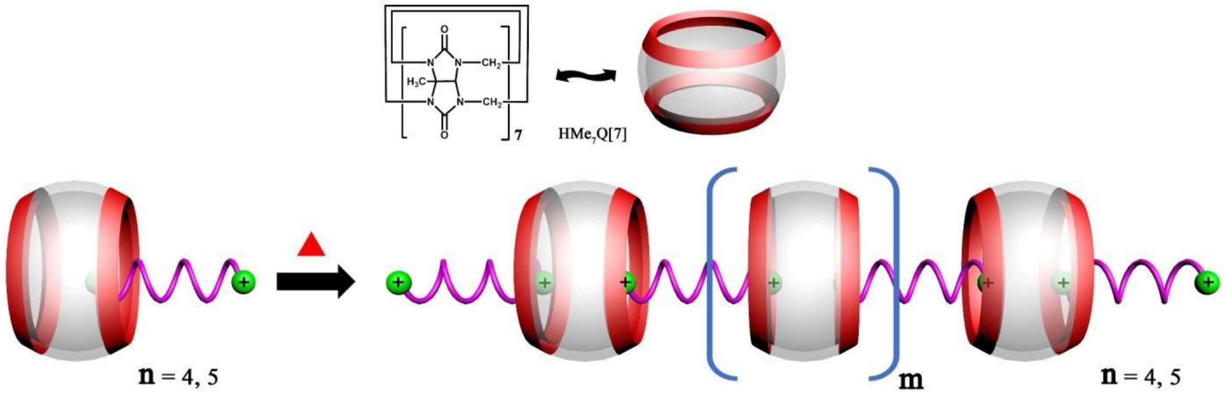

Figure 5. Supramolecular polymer aggregated from head-inclusion complex.

It is also noteworthy that ammonium ions can act as templates in Q[*n*] formation, influencing both the kinetics and the thermodynamics of the process. In particular, Anzenbacher, Jr. and Isaacs and coworkers showed that the *p*-xylylenediammonium ion was capable of acting as a template in the reaction between glycoluril and formaldehyde (< 2 equiv.) affording a methylene bridged glycoluril hexamer and bis-nor-seco-Q[10].[72] Importantly, this methodology could be readily scaled up to deliver, without the need for chromatography, multigram quantities of the hexamer. Further reaction (macrocyclization) with phthalaldehydes allowed access to monofunctionalized Q[6] derivatives, for example derivatives containing NO_2 or CO_2H motifs, thereby opening up the possibility for further functionalization. The size of the template proved crucial in determining the product formed during the macrocyclization. For example, both the *p*-xylylenediammonium and hexanediammonium ions were found to slow down the formation of Q[6], instead preferring to favour formation of an intermediate containing an NCOCN-bridge which contains two stereogenic centers. Conducting the reaction between the hexamer and *o*-phthaldehyde in CF_3CO_2H allowed the intermediate to be characterized by mass spectrometry and ^{1}H NMR spectroscopy.

Cao and Isaacs designed a monofunctionalized Q[6] derivative (symbol **1** in Figure 6) that possessed a covalently bonded (add by Click chemistry via a propargyloxy substituent) isobutylammonium group.[73] The structure comprised a mixture of cyclic dimers as evidenced by DOSY and ESI-MS experiments, and in water, they self-assemble into a cyclic daisy chain. This structure proved to be responsive to specific competing hosts, for example whilst Q[6] and Q[7] had little effect, the addition of Q[8] (1.5 equiv.) resulted in the formation of a new complex involving the monomeric isobutylammonium and Q[8]. ^{1}H NMR studies (upfield shifts for the triazole and isobutylammonium protons) indicated that back-folded conformation was present in the Q[8] cavity. Further addition of Q[6] reverses the process and gives back the daisy chain. Obviously, substituent in **1** also act as a competitive guest.

View Article Online
DOI: 10.1039/D0QI00529K

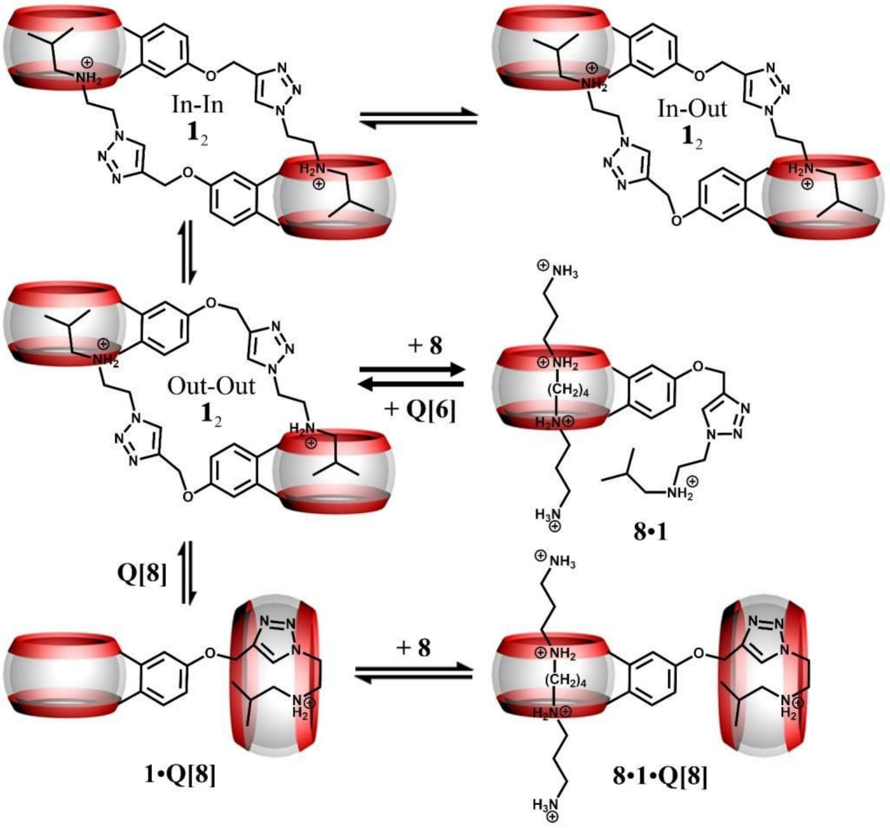

Figure 6. Depiction of the three isomers of $\mathbf{1}_2$ and their response to addition of spermine (symbol **8**), Q[8], and Q[6].

3.2 Binding behaviour of *N*-alkylated viologens with substituted Q[*n*]s

The series of *N*-alkylated viologens (methyl viologen MV^{2+}, ethyl viologen EV^{2+}, propyl viologen PV^{2+}, butyl viologen BV^{2+}, pentyl viologen FV^{2+} and heptyl viologen HV^{2+}) are special redox-active organic guests with an alkyl chain and an aromatic group. A host−guest study involving *N*-alkylated viologens can help to understand the interdependence of redox processes and molecular selectivity. We and others have performed a series of experiments to study the binding interactions between a series of *N*-alkylated viologen guests and the substituted Q[6]s, including $(HO)_1Q[7]$[55], $CyH_6Q[6]$[74], TMeQ[6][75], $CyH_2Q[6]$[76] and $CyH_3Q[6]$[76]. As shown in Figure 7, MV^{2+} and EV^{2+} form 1:1 complexes in which the bipyridinium aromatic nucleus is partially included inside the $CyH_6Q[6]$ cavity. PV^{2+}, BV^{2+},

View Article Online
DOI: 10.1039/D0QI00529K

FV^{2+}, and HV^{2+} form 2:1 complexes with CyH$_6$Q[6], in which each of the viologen aliphatic chains is included by a host molecule. The results suggested that the inclusion of the alkyl chains is favored compared to inclusion of the aromatic nucleus.[74]

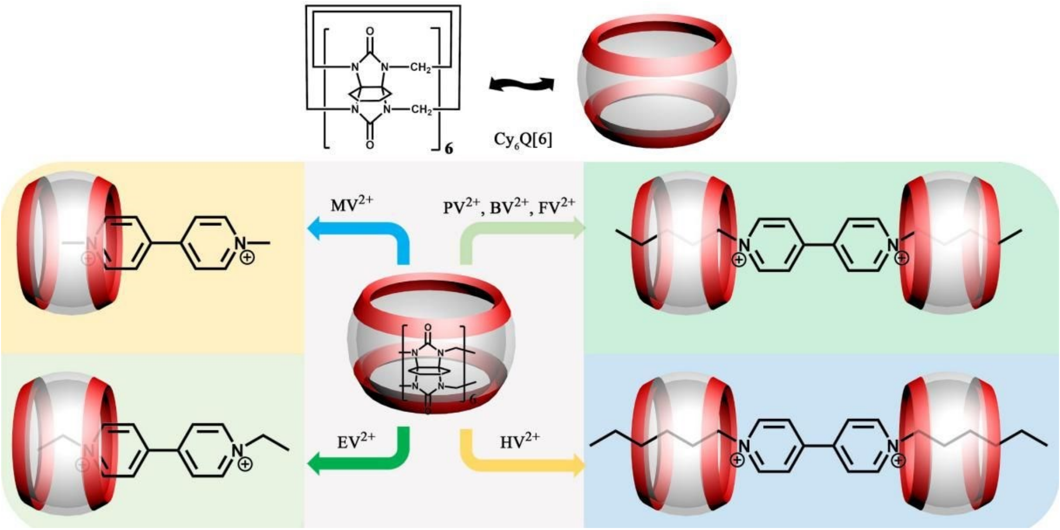

Figure 7. Binding behaviour of *N*-alkylated viologens with CyH$_6$Q[6].

3.3. Aniline-containing guests recognized by substituted Q[*n*]

In these Q[*n*] systems, it is usual to encounter shielding and deshielding effects of the host. For example, the hydrophobic cavity of a Q[*n*] is a proton-shielding region. When the guest is encapsulated into the Q[*n*] cavity, the proton signals of the guest undergo an upfield shift. In contrast, the outside of the portals of a Q[*n*] is a proton-deshielding region which would induce a downfield shift of the proton signals of guests located outside of the Q[*n*] portal. However, we recently encountered shielding and deshielding effects induced by a guest.[75-77] When the aromatic motif of a guest, such as aniline-containing guests, is located inside of the TMeQ[6] cavity, the ellipsoidal cavity of the TMeQ[6] is complementary in both size and shape to the aromatic group of the guest. As a result, remarkable chemical shifts for the TMeQ[6] host protons were observed (Figure 8). Similar situations were observed for other substituted Q[*n*]s with ellipsoidal cavity.[76]

View Article Online
DOI: 10.1039/D0QI00529K

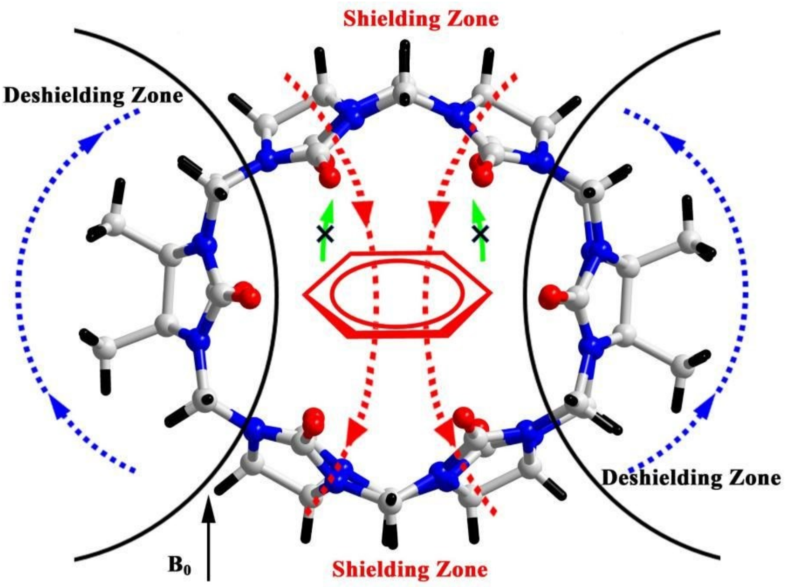

Figure 8. Aromatic ring-induced shielding and deshielding zones.

3.4. Recognition of enantiomeric amino acids by substituted Q[*n*]s

Amino acid recognition and determination is of great significance in fields as diverse as food testing, nutritional analysis, and medical diagnostics.[78–80] In 2017, we reported a family of supramolecular complexes of TMeQ[6] which interacted with enantiomeric amino acids (D,L-Gln; D, L-Glu; D,L-Met; D,L-Ser; D-Val).[81] The seven supramolecular complexes are classified into two structural types, inclusion and exclusion structures (Figure 9), the adoption of which mainly depends on the length of the alkyl chain of the enantiomeric amino acid. Interestingly, the reaction of TMeQ[6] with L-Val doesn't produces a crystalline material, suggesting that TMeQ[6] can be used to separate D-Val from its enantiomer.

View Article Online
DOI: 10.1039/D0QI00529K

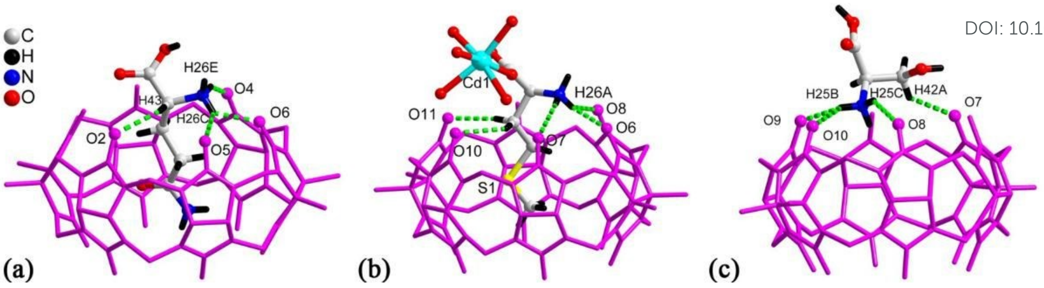

Figure 9. X-ray crystal structure of TMeQ[6] complexes with different amino acids showing inclusion and exclusion structural types.

3.5. Recognition of other organic guests by substituted Q[*n*]s

Haloalkanes are an important class of organic compound which possess various applications. In 2015, we reported the first example of haloalkane encapsulation inside the cavities of Q[*n*]s.[82] X-ray crystallography and NMR spectroscopy were used to establish that the haloalkane 1-(3-chlorophenyl)-4-(3-chloropropyl)-piperazinium (PZ^+) dihydrochloride forms a highly stable inclusion complex PZ^+@TMeQ[6], with half of the chloropropyl group of the PZ^+ residing within the TMeQ[6] cavity (Figure 10).

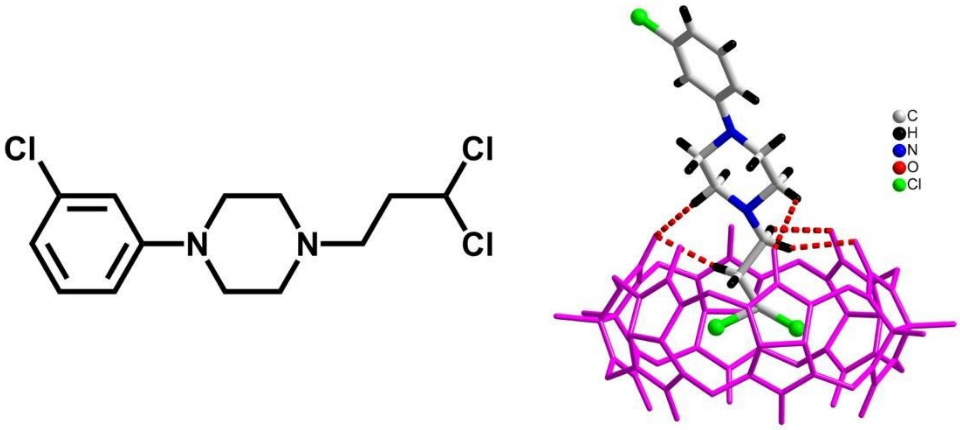

Figure 10. ORTEP diagram of the inclusion complex PZ^+@TMeQ[6].

The binding behaviour of $HMe_7Q[7]$ with 1,10-phenanthroline and its derivative 4,7-dimethyl-1,10-phenanthroline was investigated by NMR spectroscopy and ITC techniques,

View Article Online
DOI: 10.1039/D0QI00529K

which suggested the formation of a half-inclusion complex and a double binding complex (Figure 11).[83] The latter complex exhibits two binding modes simultaneously: *endo* binding and *exo* binding, which is not observed in conventional host−guest complexes.

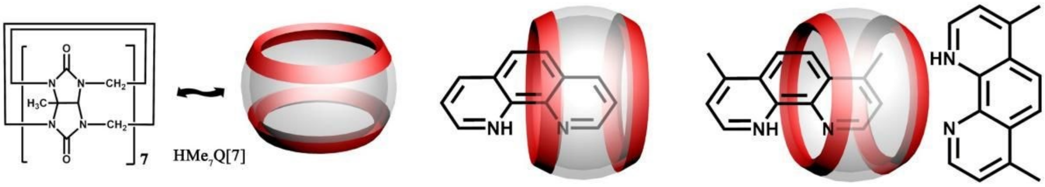

Figure 11. Schematic representation of two binding modes.

As more substituted Q[*n*]s are synthesized, more organic guests are reported to be recognized and accommodated by these new substituted Q[*n*]s. For example, hymexazol[84], thiabendazole[85], 6-benzyladenine[86] were reported to form inclusion complexes with $HMe_6Q[6]$, and TMeQ[6]. Kaifer, Dong and coworkers recently studied the binding properties of $(HO)_1Q[7]$ with a series of selected guests.[55] The results indicated that the binding affinities of the guests with the $(HO)_1Q[7]$ were slightly smaller than those of the parent Q[7].

4. Coordination chemistry of substituted Q[*n*]s with metal ions

The two identical carbonyl-laced portals that Q[*n*]s possess makes them fascinating coordination ligands. The coordination affinities of substituted Q[*n*]s are different from those of their parent Q[*n*]s because of the effects of the substituents. This is in part due to the new affinities displayed by the introduced substituents, which will become evident from the examples described below, but also because these substituents impart new properties such as increased solubility which can greatly enhance chemical reactivity. For fully and partially alkyl-substituted Q[*n*]s, the alkyl groups on the waist belong to electron-donating groups, which can enhance the polar properties of the carbonyl oxygen atoms at the portal, and enhance the

View Article Online
DOI: 10.1039/D0QI00529K

electrostatic interactions between substituted Q[*n*]s and metal ions. In this section, we describe the outstanding coordination properties of the substituted Q[*n*]s, and their coordination compounds with a wide range of metal ions, including alkali metals, alkaline-earth metals, transition metals and lanthanides. These coordination compounds (Table 2) have led to many interesting structural features and applications, some of which are discussed herein.

4.1. with alkali metal ions

Generally, the coordination of Q[*n*] homologues with alkali metal ions leads to discrete (closed or opened) molecular capsules or 1D chains because the Q[*n*] homologues contains only two opposite coordination orientations. For instance, we previously reported a series of discrete molecular capsules of unsubstituted Q[5] with various metal ions, such as alkali (K^+), alkaline earth (Ba^{2+}), transition (Cd^{2+}), and lanthanide (La^{3+}) metal ions.[87] However, $(HO)_mQ[n]$ are a series of multi-dentate ligands with different coordination orientations. In 2011, we prepared and characterized three coordination polymers of alkali metal ions (K^+, Rb^+ and Cs^+) with the $(HO)_{10}Q[5]$ ligand.[88] Their crystal structures revealed that not only the carbonyl groups of the portals but also the hydroxy groups at the waist position of the $(HO)_{10}Q[5]$ ligand participated in the coordination, which led to 1D to 2D coordination polymers **A-1-3** (Figure 12).

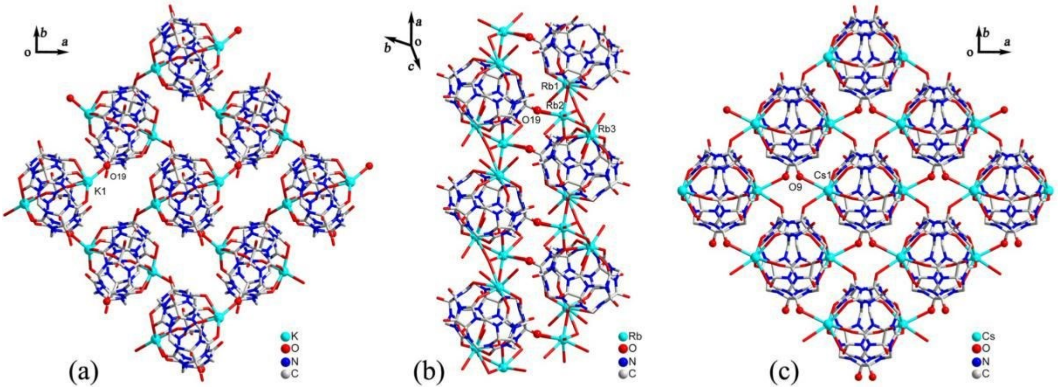

Figure 12. 2D coordination polymers of $(HO)_{10}Q[5]$ with alkali metal ions (K^+, Rb^+ and Cs^+).

In 2008 and 2010, Day, Lindoy, Tao, and Wei *et al.* reported three attractive catenane

View Article Online
DOI: 10.1039/D0QI00529K

structures, which resulted from the coordination of three substituted Q[5]s (1,2,4-$Me_3Q[5]$, 1,2,4-$CyH_3Q[5]$ and $CyH_5Q[5]$) with potassium ions.[89,90] These catenated structures **A-5-7** featured trigonal-planar units, each one involving three substituted Q[5] ligands and six bound K^+ ions. Adjacent trigonal-planar basic units connected with each other through their bound K^+ ions, generating a 10-ligand "bracelet" framework. Interpenetration of the "bracelet" framework led to a complicated 3D catenane structure (Figure 13). Using a similar strategy, Tao group also prepared a series of 2D networks **A-8-12** by using the coordination of K^+ ion with other substituted Q[5]s, including $Me_2Q[5]$, 1,3-$CyH_2Q[5]$, 1,2,3-$CyH_3Q[5]$ and 1,2,4-$CyH_3Q[5]$.[91] Apparently, the electron donating effect of the substituents increased the electron density at the portals of these substituted Q[5] ligands, and hence enhanced their binding affinities.

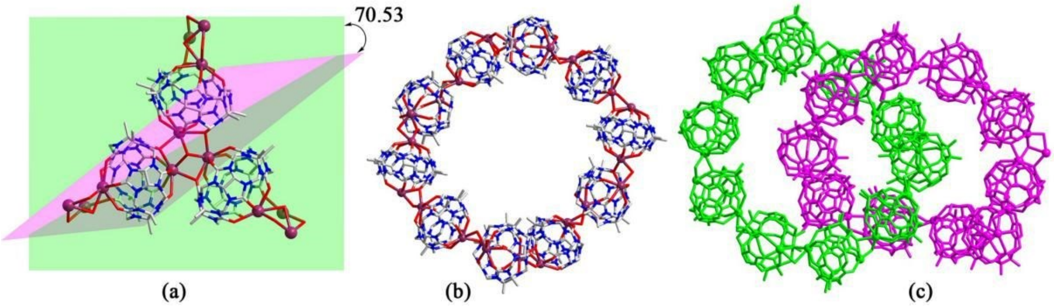

Figure 13. (a) Schematic illustrating that the dihedrals between any two K1 junction planes in the trigonal planar branch are identical at 70.53; (b) A single 10-membered 1,2,4-HMeQ[5] "bracelet"; (c) Catenation of two 10-membered 1,2,4-HMeQ[5] bracelets.

We and others have also reported coordination compounds of alkali metal ions (Na^+, K^+, Rb^+ and Cs^+) with both fully and partially alkyl-substituted Q[*n*]s, including TMeQ[6][92], $Me_{10}Q[5]$[93–95], $CyP_5Q[5]$[96], OMeQ[6][97], $(HO)_1OMeQ[6]$[98], 1,3,5-Me6Q[6][99]. For example, Chen, Tao and coworkers investigated the coordination of OMeQ[6] with alkali metal ions in the presence of polychloride cadmium anions, such as $[Cd_2Cl_8]^{4-}$, $[CdCl_4]^{2-}$, and $[Cd_2Cl_7]^{3-}$ anions, or in the presence of *p*-hydroxybenzoic acid.[97] The resulting structures **A-29-34**

View Article Online
DOI: 10.1039/D0QI00529K

indicated the presence of "outer-surface interactions", which are a unique type of noncovalent interaction first proposed by Tao.[100] For the OMeQ[6] molecules and the selected inorganic anions or aromatic molecules (Figure 14), such interactions play an important role in the formation of different OMeQ[6]/A^+-based supramolecular assemblies.

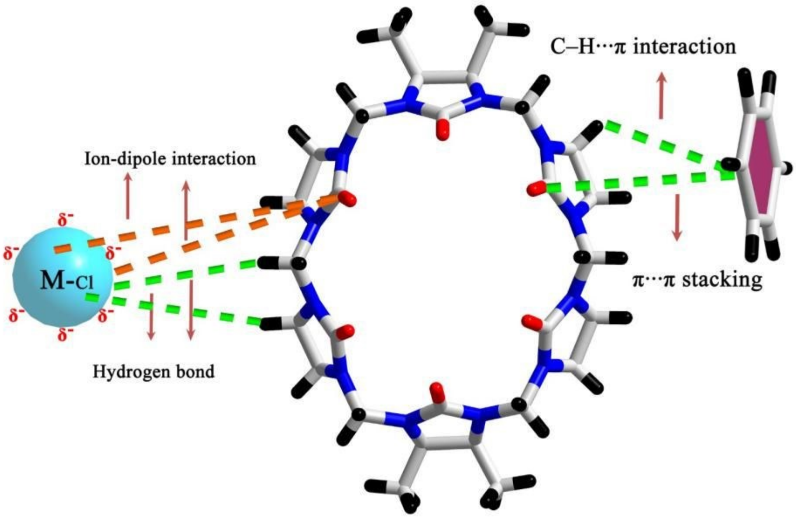

Figure 14 Outer-surface interactions of OMeQ[6] with inorganic anions (left) and aromatic moieties (right).

4.2. Interaction with alkaline earth metal ions

As early as 2008, Tao group reported the coordination compounds **AE-5** and **AE-6** of TMeQ[6] which incorporated two alkaline earth metal ions, Ca^{2+} and Sr^{2+}, which coordinated directly to the TMeQ[6] ligand.[101] In 2012, we prepared and characterized three coordination compounds **AE-7-9** of the $CyH_5Q[5]$ ligand with alkaline-earth metal ions (Ca^{2+}, Sr^{2+}, Ba^{2+}).[102] Analysis of the crystallographic data indicated that the radius (size) of the coordinated metal ions determines whether the molecular capsule is closed or opened (Figure 15).

View Article Online
DOI: 10.1039/D0QI00529K

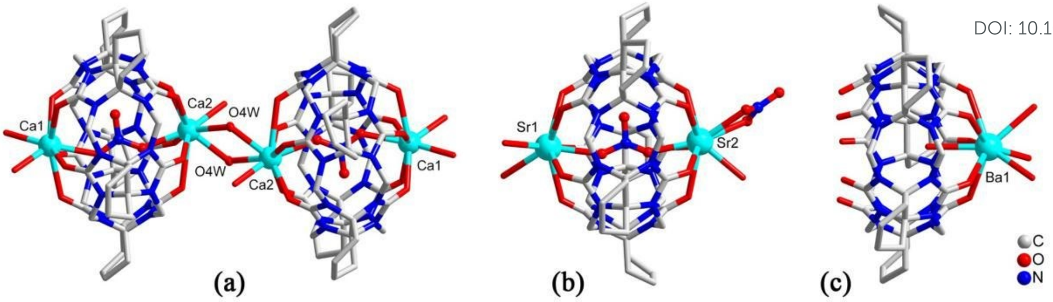

Figure 15 Crystal structures of three coordination compounds of CyH$_5$Q[5] with alkaline-earth metal ions (Ca^{2+}, Sr^{2+} and Ba^{2+}) showing three kinds of molecular capsules.

Tao and Ma *et al*. investigated the coordination compounds **AE-10-17** of CyP$_5$Q[5] and CyP$_6$Q[6] with a series alkaline-earth metal ions (AE^{2+} = Mg^{2+}, Ca^{2+}, Sr^{2+}, Ba^{2+}) in the presence of [ZnCl$_4$]$^{2-}$ anions.[103,104] X-ray diffraction analysis revealed that the [ZnCl$_4$]$^{2-}$ anion acts as an inducer in the self-assembly of the CyP$_5$Q[5]/CyP$_6$Q[6]-based complexes. As shown in Figure 16, for example, due to the ion−dipole interaction between the [ZnCl$_4$]$^{2-}$ anions and the electropositive outer surface of the CyP$_5$Q[5], the [ZnCl$_4$]$^{2-}$ anions form a honeycomb-like framework, and the CyP$_5$Q[5]-Mg^{2+} coordination complex occupy the cells of this framework. For coordination compounds of alkaline earth metal ions with other substituted Q[*n*]s, such as (HO)$_1$OMeQ[6][99], *o*-TMeQ[6][41], CyP6Q[6][104], HMe6Q[6][105] and (HO)$_1$Q[7][106], the honeycomb effect is also observed, which originates from the inorganic anions [CdCl$_4$]$^{2-}$ or [ZnCl$_4$]$^{2-}$.

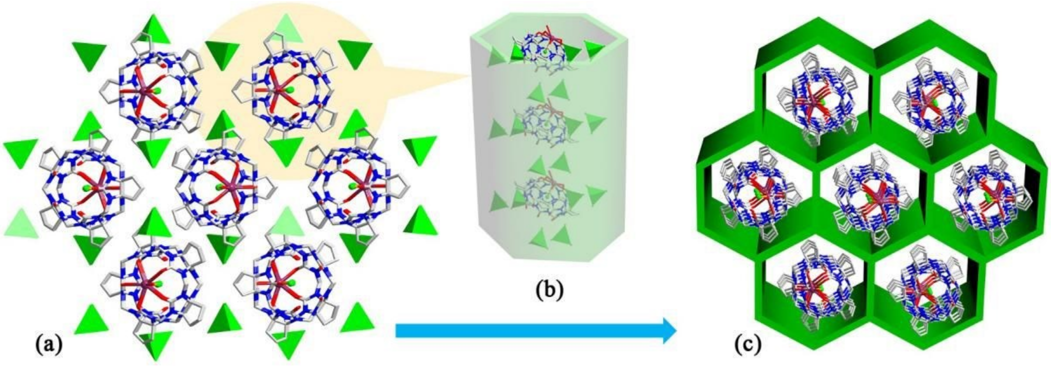

Figure 16 Binding interaction of Mg^{2+} with CyP$_5$Q[5]. (a) Supramolecular assembly of Mg^{2+} cations,

DOI: 10.1039/D0QI00529K

$CyP_5Q[5]$ molecules and $[ZnCl_4]^{2-}$ anions. (b) Occupying the cells of the framework. (c) Honeycomb-like framework constructed of $[ZnCl_4]^{2-}$ anions, with $CyP_5Q[5]$-based chains.

Coordination compounds of substituted Q[*n*]s with alkaline-earth metal ions constructed in the presence of inorganic anions usually possess different porous structures, and display differing absorption of volatile compounds.[103,105,106] For example, the $HMe_6Q[6]$-Ca^{2+}/Ba^{2+}-$[CdCl_4]^{2-}$–based coordination compounds **AE-18** and **AE-19** exhibit excellent thermal stability as well as permanent porosity. They also show high adsorption capacity and selectivity to Et_2O and CH_3OH.[105] The porous materials constructed by the coordination compounds of $(HO)_1Q[7]$ with Ca^{2+} and Sr^{2+}, **AE-20** and **AE-21,** revealed a large sorption capacity for CH_3OH.

4.3. Interaction with transition metal ions

Transition metal coordination complexes usually display special optical, electrical and magnetic properties. However, only a few examples of Q[*n*]-transition metal coordination complex have been reported.[107–110] More often than not, transition metal ions prefer to form aqua complexes rather than to coordinate with Q[*n*] ligands in aqueous solution. This section presents some examples of substituted Q[*n*]s complexes with transition metal ions.

In 2010, the complexation behaviour of $CyH_6Q[6]$ with Cd^{2+} ions was investigated by electrochemical methods and X-ray crystallography.[108] The host $CyH_6Q[6]$ displayed extraordinary binding affinity towards Cd^{2+} ions. It can form a 1:6 $CyH_6Q[6]$/Cd^{2+} complex **TM-1** in both aqueous solution and the solid state (Figure 17). The strong binding affinity of $CyH_6Q[6]$ toward Cd^{2+} ions may be derived from to the electron donating property of its six substituted cyclohexano groups. The study suggests the potential utility of $CyH_6Q[6]$ as an effective chelator and extractant for toxic heavy metals.

View Article Online
DOI: 10.1039/D0QI00529K

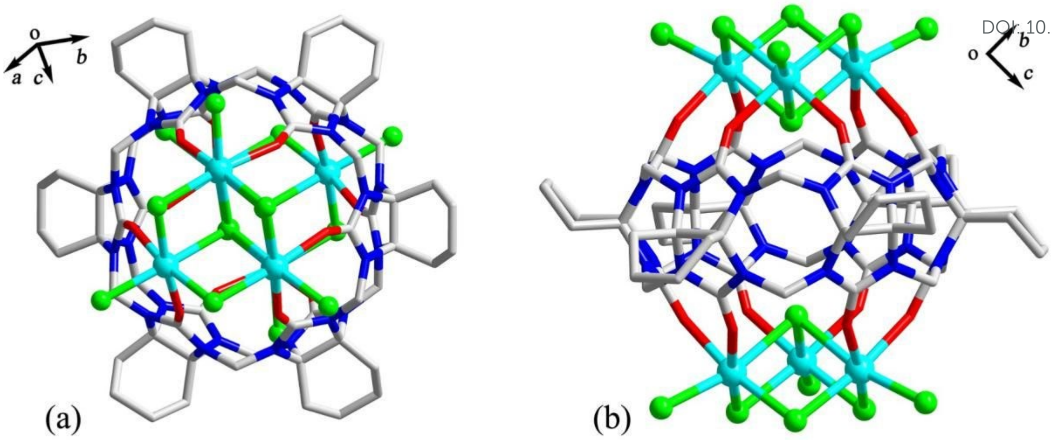

Figure 17 X-ray structure of CyH$_6$Q[6]/Cd^{2+} complex: (a) top view; (b) side view.

Three years later, we studied the effect of chloride anion concentration on the self-assembly of supramolecular architectures based on TMeQ[6] and copper chloride.[109] Under different chloride anion concentrations, three supramolecular architectures **TM-2-4** were obtained through the reaction of TMeQ[6] and copper chloride. X-ray diffraction analysis revealed three tubular structures (Figure 18), one of which is attributed to coordination bonds and the other two resulted from weak noncovalent interactions. In 2013, Zhang *et al.* described coordination compounds of CyP$_6$Q[6] (**TM-5**) and TMeQ[6] (**TM-6-8**) with Cu^{2+} in the absence or presence of a third species.[110] The resulted coordination compounds showed how the corresponding supramolecular assemblies can depend on the addition of the third species. Very recently, Ma and co-workers studied coordination compounds of CyP$_5$Q[5] (**TM-9** and **TM-10**) and CyP$_6$Q[6] (**TM-11** and **TM-12**) with two transition metal ions, namely Cu^{2+} and Zn^{2+}.[111]

View Article Online
DOI: 10.1039/D0QI00529K

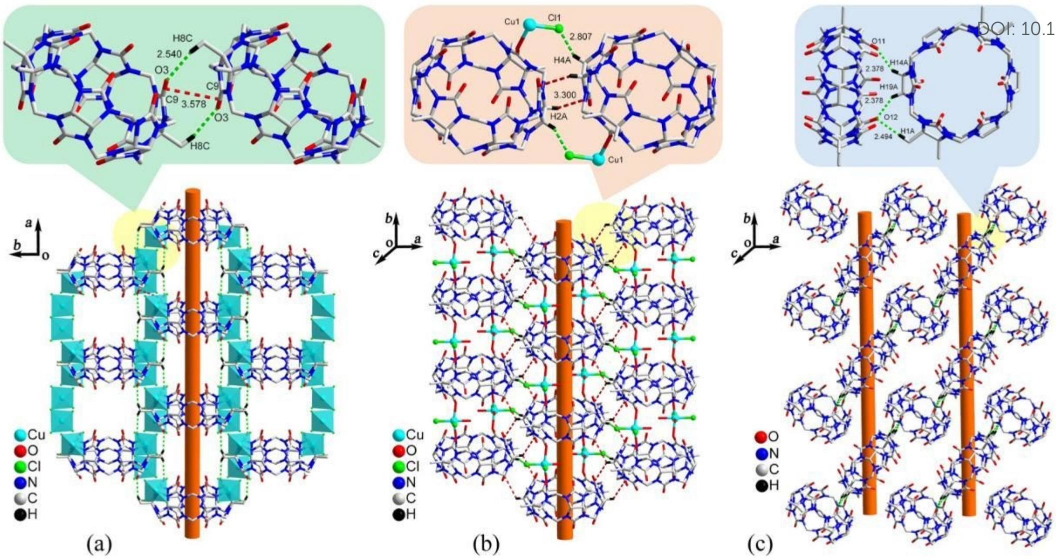

Figure 18 Three tubular structures self-assembled from TMeQ[6] and copper chloride under different chloride anion concentrations.

4.4. Interaction with lanthanide metal ions

Due to their unique physicochemical properties, lanthanide ions are widely used in numerous technological devices.[112–114] However, lanthanide ions are difficult to separate because of the poor shielding of the nuclear charge by filling of the 4f electron shell. The study of lanthanide coordination complexes here may lead to fascinating topological structures and promising applications. On comparison with other metal ions, lanthanide ions are the most studied in the coordination chemistry of substituted Q[*n*]s.[115–123]

Because of the effect of lanthanide contraction, the lanthanide complexes with substituted Q[*n*]s usually display interesting structural progressions. As early as 2012, we prepared eight coordination compounds **Ln-1-8** of $CyH_5Q[5]$ with a number of lanthanide ions (La^{3+}, Ce^{3+}, Pr^{3+}, Nd^{3+}, Sm^{3+}, Dy^{3+}, Ho^{3+}, and Er^{3+}) by reactions of the corresponding lanthanide species with the $CyH_5Q[5]$ in aqueous solution.[115] Crystal structure analysis revealed two coordination modes (Figure 19). Close inspection of these crystal structures revealed some interesting structural variations, which were ascribed to the effect of lanthanide contraction.

View Article Online
DOI: 10.1039/D0QI00529K

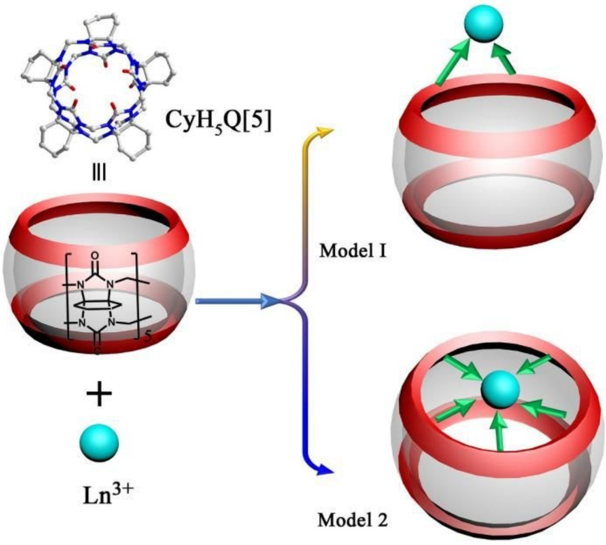

Figure 19 Two kinds of coordination mode observed for $CyH_5Q[5]$ with lanthanide ions.

In the following year, the effect of lanthanide contraction induced coordination architectures of $CyH_6Q[6]$ was also studied by Ni and Tao *et al.*[116] The slightly different ionic radii of the lanthanide metal ions plays a key role in the formation of different coordination modes for $CyH_6Q[6]$. As a result, fifteen coordination architectures **Ln-9-23** of $CyH_6Q[6]$-Ln were structurally classified into four groups, as shown in Figure 20.

On the other hand, each substituted Q[*n*] displays a different binding affinity to the same lanthanide ions. Some substituted Q[*n*]s only coordinate with light lanthanide ions, while others only coordinate with heavy lanthanide ions, and this provided a new method for separating lanthanide ions. For example, Zhu *et al.* investigated the interactions between a series of lanthanide ions and $HMe_5Q[5]$ and $HMe_6Q[6]$ in 2015.[117] X-ray diffraction analysis revealed that $HMe_5Q[5]$ and $HMe_6Q[6]$ selectively interacted with certain lanthanide ions. In the presence of $[CdCl_4]^{2-}$, $HMe_5Q[5]$ crystallized with four light lanthanides, La^{3+}, Ce^{3+}, Pr^{3+}, and Nd^{3+} and formed the coordination capsules **Ln-24-27**, whereas the other lanthanide ions remained in solution. Under the same conditions, $HMe_6Q[6]$ crystallized with aqua complexes of lanthanide cations ($[Ln(H_2O)_8]^{3+}$, Ln = Gd–Lu) and formed the adducts **Ln-28-32**, whilst La^{3+}, Ce^{3+}, Pr^{3+}, Nd^{3+}, Sm^{3+}, and Eu^{3+} remained in solution. It should be noted that no

View Article Online
DOI: 10.1039/D0QI00529K

satisfactory data were collected for the ions Gd^{3+}, Yb^{3+}, and Lu^{3+}. In neutral solution and in the absence of $CdCl_2$, $HMe_6Q[6]$ crystallized with aqua complexes of lanthanide cations (Ln = Sm–Lu) to form adducts. Here, **Ln-33** is a representative adduct. No solid crystals of $HMe_6Q[6]$ with La^{3+}, Ce^{3+}, Pr^{3+}, and Nd^{3+} could be obtained. Energy-dispersive spectrometry (EDS) studies indicated that the lighter or heavier lanthanide ions could be isolated from their counterparts through the interaction with $HMe_5Q[5]$ and $HMe_6Q[6]$.

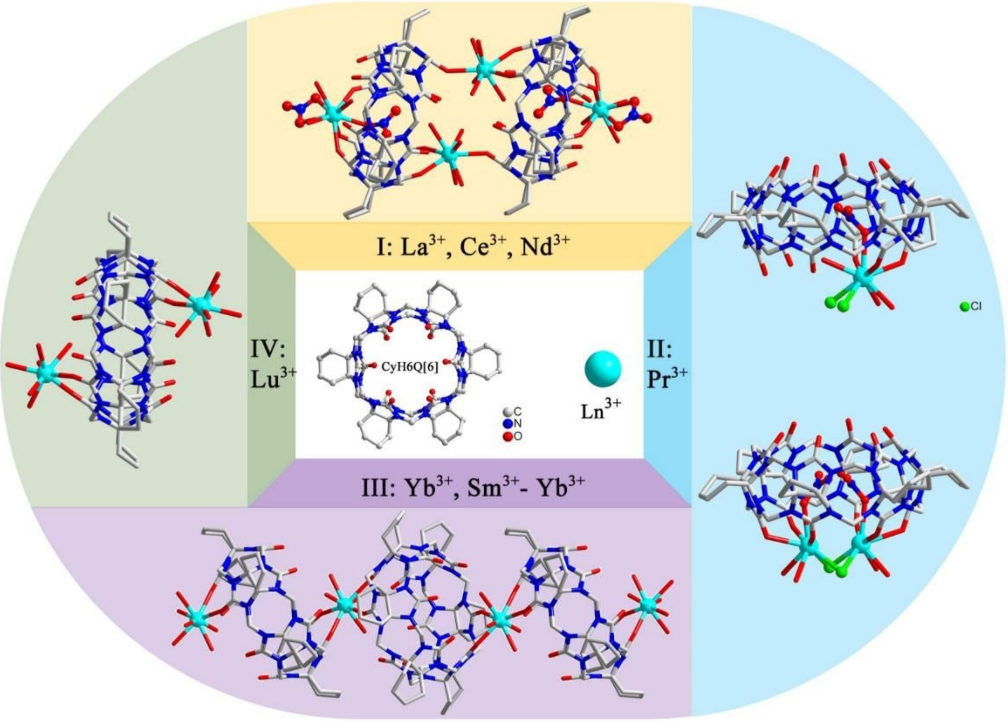

Figure 20 Coordination complexes of Cy6Q[6] with lanthanide ions, which were structurally classified into four groups.

In the past five years, the coordination chemistry of lanthanide metal ions with other substituted Q[*n*]s, such as *o*-TMeQ[6][118,122], OMeQ[6][119], CyP6Q[6][120], *t*$(HO)_2$OMeQ[6][121], and CyH6Q[6][123], under different conditions were also studied. Table 3 lists the coordination conditions and results of all substituted Q[*n*]s on interaction with lanthanide metal ions.

View Article Online
DOI: 10.1039/D0QI00529K

5. Applications of substituted Q[*n*]s

It must be noted that applications of hydroxylated Q[*n*]s and their derivatives have been reviewed in our previous work[19], and will not be discussed in this review.

5.1. Catalysis

In 2013, the Cao group prepared a series of M-Pd-$Me_{10}Q[5]$ (M=Li, Na, K, Rb, and Cs) hybrid solid materials (Figure 21), which displayed excellent catalytic performance and good recyclability as phosphine-free pre-catalysts for Heck cross-coupling reactions.[124] Their studies revealed that the activated Pd(II) species were released from the crystalline hybrid pre-catalysts and were transformed into catalytically active Pd nanoparticles during the catalytic reactions. In the following year, the Cao group prepared a composite material Ag@$Me_{10}Q[5]$, in which spherical silver nanoparticles (Ag^0 NPs) with an average size of *ca*. 4.4 nm was observed.[125] As a heterogeneous catalyst for the reduction of various nitrophenols, the composite material Ag@$Me_{10}Q[5]$ exhibited excellent catalytic performance and remained active after several consecutive cycles.

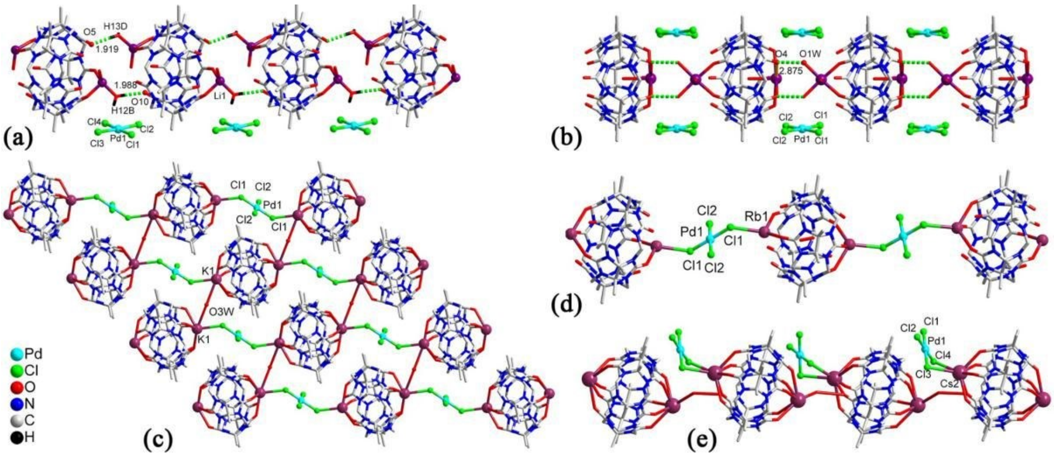

Figure 21 Crystal structures of a series of M-Pd-$Me_{10}Q[5]$ (M=Li, Na, K, Rb, and Cs) hybrid solid materials.

5.2. Inorganic-organic hybrid materials

View Article Online
DOI: 10.1039/D0QI00529K

The redox catalysis and magnetism exhibited by inorganic polyoxometalates (POMs) has made them attractive for research.[126] In 2009, Kögerler and coworkers reported an example of a hybrid supramolecular architecture based on POMs and Q[*n*].[127] Since then, Cao, Tao, Zhang, Zhu and co-workers have demonstrated numerous hybrid compounds of POMs with substituted Q[*n*] derivatives.[128–137] Very recently, Zhang and co-workers found that the self-assembly of $(HO)_{12}Q[6]$ and Keggin-type POMs (such as $H_3[PMo_{12}O_{40}]$ and $H_3[PW_{12}O_{40}]$) under different concentrations of hydrochloric acid yields two types of supramolecular assemblies: one being hybrid compounds $(HO)_{12}Q[6]$-POMs-HCl and the other $(HO)_{12}Q[6]$-HCl (Figure 22).[137]

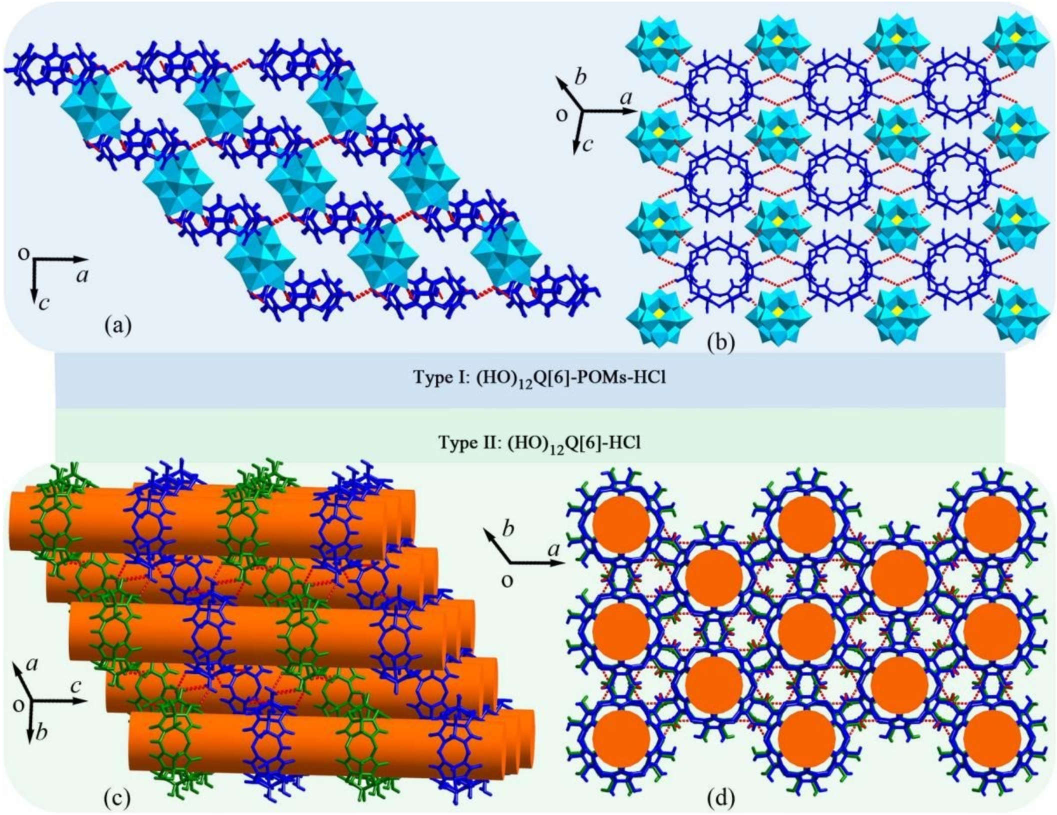

Figure 22 Two types of supramolecular assemblies, hybrid compounds $(HO)_{12}Q[6]$-POMs-HCl and accumulation body of $(HO)_{12}Q[6]$-HCl.

They exhibited various interesting chemical and physical properties. It is worth mentioning that the complexation of POMs with Q[*n*]s or substituted Q[*n*]s is driven by “outer-surface interactions”, including ion−dipole interactions, hydrogen bonding, C-H···π interactions, as well

View Article Online
DOI: 10.1039/D0QI00529K

as π···π stacking. Compared to Q[*n*]s, HO groups of the $(HO)_{12}Q[6]$ facilitate the formation of the "outer-surface interactions", and enhance crystal stability of the supramolecular assemblies.

5.3. Fluorescent chemosensors

Using the host−guest interactions of TMeQ[6] and $HMe_6Q[6]$ with a fluorophore guest (Figure 23) as a fluorescence indicator displacement (FID) system, Ni and co-workers constructed a new type of ratiometric fluorescent chemosensor for the sensing, detection, and recognition of two α-amino acids, namely lysine and methionine.[138] As indicated in Figure 23, the differing binding interactions of the two substituted Q[6]s towards the target analytes led to a useful ratiometric detection signal output for the discrimination of lysine and methionine *versus* the other tested α-amino acids.

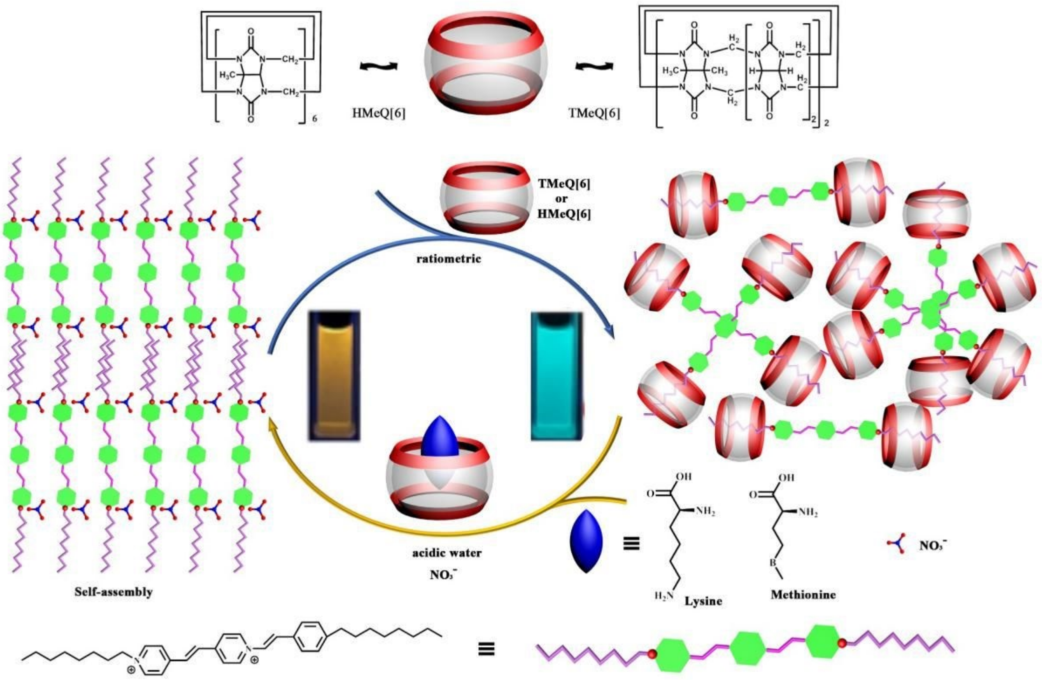

Figure 23. Illustration of the plausible fluorescence indicator displacement process based on host−guest interactions.

View Article Online
DOI: 10.1039/D0QI00529K

As part of their template studies (see section 3.1), Anzenbacher, Jr. and Isaacs and coworkers isolated a Q[6] derivative with a covalently attached 2,3-dialkylnaphthalene fluorophore (symbol **19** in Figure 24), which can emits fluorescence in response to UV irradiation.[72] When combined with a number of different metals, only in the case of Eu^{3+} or Dy^{3+} was significant fluorescence quenching observed. The Eu^{3+} system was found to act as a sensor for the histamine shown below (Figure 24, bottom, left). It was postulated that the histamine occupies the cavity and one ureidyl C=O portal and adopts a 1:1 binding model; the Eu^{3+} was thought to occupy the other ureidyl C=O portal. The addition of the histamine leads to displacement of the quenching Eu^{3+} or Dy^{3+}, and recovers fluorescence.

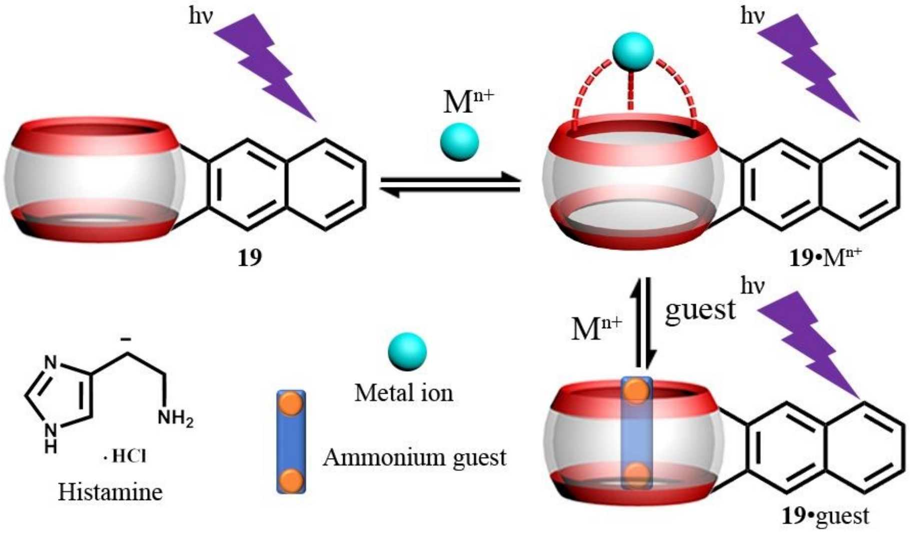

Figure 24. Structure and Schematic representation of fluorescence assay based on **19**.[72]

Urbach and coworkers reported an optical sensor based on the combination of Q[7] and tetramethylrhodamine.[139] Equilibrium dissociation constants for this system matched those of the parent Q[7] despite the presence of the fluorophore. Cellular uptake was demonstrated using HT22 neurons, with localization at the cytoplasm and no disruption of cell growth over a 4 day period (concentration ≤2.2 μM).

View Article Online
DOI: 10.1039/D0QI00529K

5.4. Controlled "smart" SERS hot spot

One of the challenges that has faced single-molecule surface-enhanced Raman spectroscopy (SERS) is the ability to place the single molecule of interest reliably within a hot spot. In their pioneering work, Kim and co-workers demonstrated a novel strategy for locating and securing a single target analyte in a SERS hot spot at a plasmonic nanojunction.[140] As shown in Figure 25, a thiol-functionalized cucurbit[6]uril, mercaptopropyloxy-Q[6] (thiol-Q[6]), acts as dual-function building block: a molecular spacer to generate a nanogap between a Ag nanoparticle and a Ag substrate, and a binding pocket to accommodate the target molecule through host−guest interactions. It is noteworthy that the substituent of the thiol-Q[6] play an important role in linking single silver nanoparticle (AgNP) to Ag substrate. The position of the hot spot is controllable by adjusting the length of the polymethylene linker separating the target from the binding moiety, spermine.

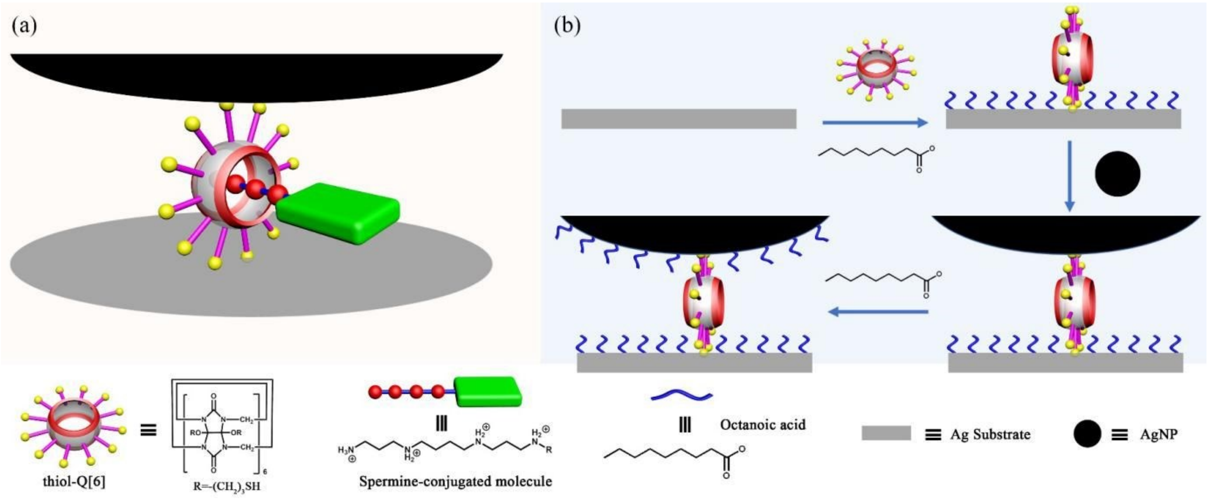

Figure 25 (a) Schematic representation of a SERS hot spot; (b) Fabrication process of a SERS hot spot.

5.5. Gas inclusion and adsorption

View Article Online
DOI: 10.1039/D0QI00529K

Huber *et al.* recently investigated the binding of three substituted Q[5]s with dioxygen O_2.[141] The study revealed that the $(HO)_{10}Q[5]$ is able to significantly bind dioxygen gas at physiological temperature, even in the presence of sodium chloride at the concentration of injectable solution in blood. The study suggests the potential utility of $(HO)_{10}Q[5]$ as a precursor host to transport O_2 in a hemoglobin substitute solution.

We recently compared the binding abilities of the hosts $CyH_2Q[6]$ and $CyH_6Q[6]$ with the guests aniline, *p*-methylaniline, and *p*-phenyldiamine.[142] The results suggested that both hosts can accommodate all guests to form stable inclusion complexes. Entrapment tests and thermogravimetric analyses showed that the $CyH_2Q[6]$ possessed higher removal efficiency for aniline than did the $CyH_6Q[6]$. Presumably the size and shape of the $CyH_2Q[6]$ is more complementary to the aromatic rings of the guests than those of $CyH_6Q[6]$ (Figure 26).

Figure 26 X-ray crystal structures of $CyH_2Q[6]$ with guests aniline, *p*-methylaniline, and *p*-phenyldiamine.

In 2015, Tao group synthesized $HMe_5Q[5]$-Hydroquinone-based[143] and $HMe_6Q[6]$-based[144] supramolecular assemblies which had large porous structures. These porous materials demonstrated selective sorption for methanol and ethanol. Zhang and Chen *et al.* recently prepared two supramolecular assemblies of $(HO)_{12}Q[6]$ under different concentrations of hydrochloric acid, which were found to possess different kinds of channels.[145] These activated desolvated $(HO)_{12}Q[6]$-based solid supramolecular assemblies demonstrated high absorption

View Article Online
DOI: 10.1039/D0QI00529K

selectivities and capacities for polychloromethanes, including tetrachloromethane, trichloromethane, and dichloromethane.

6. Self-Assembly Processes using substituted Q[*n*]s

6.1. Self-Assembly of (Pseudo)rotaxane and Poly(pseudo)rotaxane

(Pseudo)rotaxanes, poly(pseudo)rotaxanes, catenanes, dentrimers, and other MIMs have attracted much attention because they are precursors for molecular machines. From a structural point of view, Q[*n*]s and substituted Q[*n*]s are perfect candidates for MIMs because they possess different hydrophobic cavities and different binding affinities. About twenty years ago, Kim and co-workers demonstrated a useful approach for constructing polyrotaxanes.[146] By using the same approach with minor modifications, some examples of MIMs based on substituted Q[*n*]s have been reported.

In 2011, we presented a novel strategy for synthesizing chiral helical polyrotaxanes. The achiral *N,N'*-bis(2-pyridylmethyl)-1,6-hexanediamine "string" contains two typical functional pyridyl groups and one 1,6-hexanediamine chain.[147] In aqueous solution, the TMeQ[6] bead was held in the middle position of the "string". The addition of $AgNO_3$ resulted in a helical polyrotaxane, which was characterized by X-ray crystallography (Figure 27).[148] The chirality of the polyrotaxane originated from the twist of the long alkyl chain when bound within the TMeQ[6] cavity. Two opposite chiral helical polyrotaxanes were observed in the crystal structure, indicating that they crystallized as a racemic compound. When KI was added to the solution of helical polyrotaxane, a mass of white precipitate was formed immediately and all of the ^{1}H NMR signals of the helical polyrotaxane disappeared, indicating that the polyrotaxane structure was thoroughly destroyed.

View Article Online
DOI: 10.1039/D0QI00529K

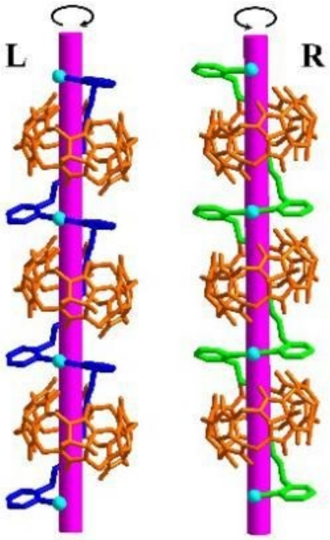

Figure 27 X-ray crystal structure of helical polyrotaxanes of TMeQ[6] with *N,N'*-bis(2-pyridylmethyl)-1,6-hexanediamine and Ag^{+}.

Zhang *et al.* reported the synthesis of two polyrotaxanes by using TMeQ[6] (Figure 28).[149] The TMeQ[6] "bead" first reacted with the "string"s of *N*,*N*′-bis(3-pyridylmethyl)-1,4 -butanediamine dichloride and *N*,*N*′-bis(3-pyridylmethyl)-1,6-hexane-diamine dichloride to form stable pseudorotaxanes. The reaction of the pseudorotaxanes with various transition metal ion Cd^{2+} then produced 1D polyrotaxanes. Another kind of polypseudorotaxanes, which involve the combination of multiple noncovalent interactions, including host−guest interactions, π–π stacking interactions, C–H···π interactions and metal–host coordination, were also reported.[150]

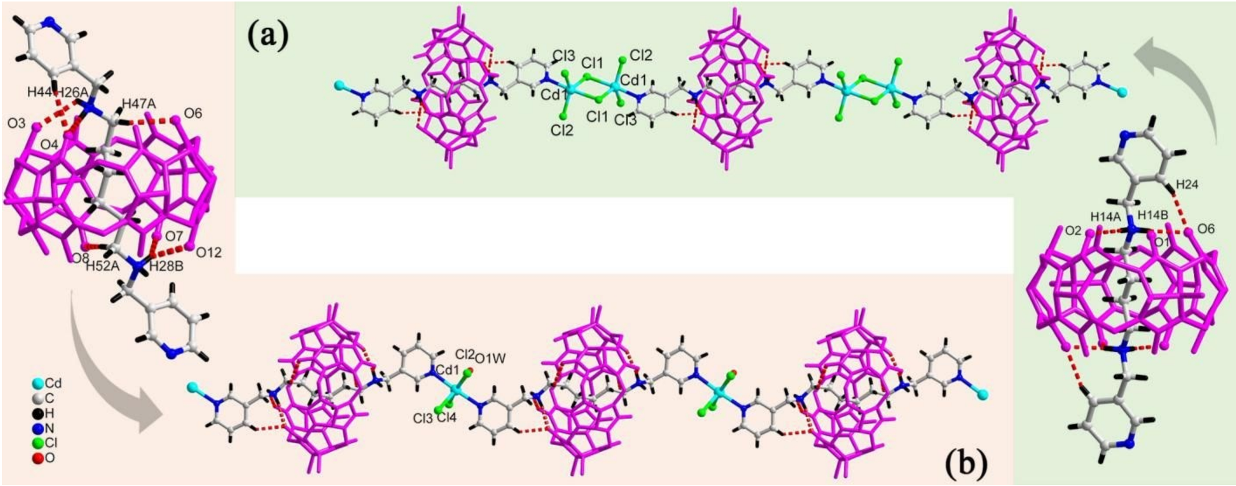

View Article Online
DOI: 10.1039/D0QI00529K

Figure 28. X-ray crystal structure of two polyrotaxanes of TMeQ[6] with *N*,*N*′-bis(3-pyridylmethyl)-1,4-butanediamine and *N*,*N*′-bis(3-pyridylmethyl)-1,6-hexane-diamine.

6.2. Self-Assembly of heterowheel pseudorotaxanes

The Day group designed and synthesized an intriguing tetraammonium chain, which performs the molecular machine function of contraction and expansion when bound with $CyP_6Q[6]$ and Q[7], respectively.[151] They also demonstrated the construction of a hetero-[4]-pseudorotaxane (Figure 29), which combined the binding function of the "wheels" $CyP_6Q[6]$ and Q[7] with the designed molecular "axle".

Very recently, we constructed two novel heterowheel [4]pseudorotaxanes consisting of TMeQ[6] and Q[7] in which the Q[7] can rotate freely around the horizontal axis, while the TMeQ[6] cannot. In the construction process of the [4]pseudorotaxanes, the dethreading and movement of the wheels along the axle was observed (Figure 30).[152] Under alkaline conditions, the [4]pseudorotaxanes is destroyed. Thus, the construction and dissociation of the [4]pseudorotaxanes can be controlled through acid/base regulation.

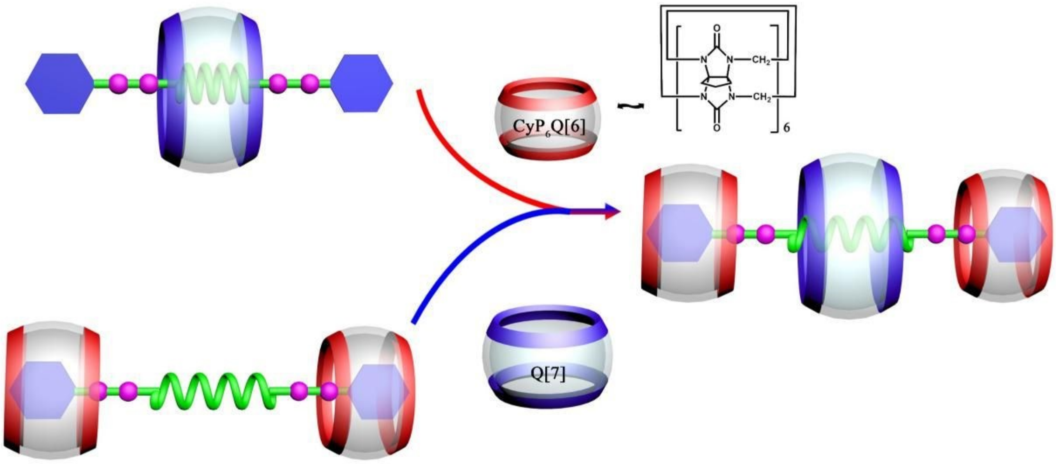

Figure 29 Schematic representation of the construction of a hetero[4]pseudorotaxane based on $CyP_6Q[6]$ and Q[7].

View Article Online
DOI: 10.1039/D0QI00529K

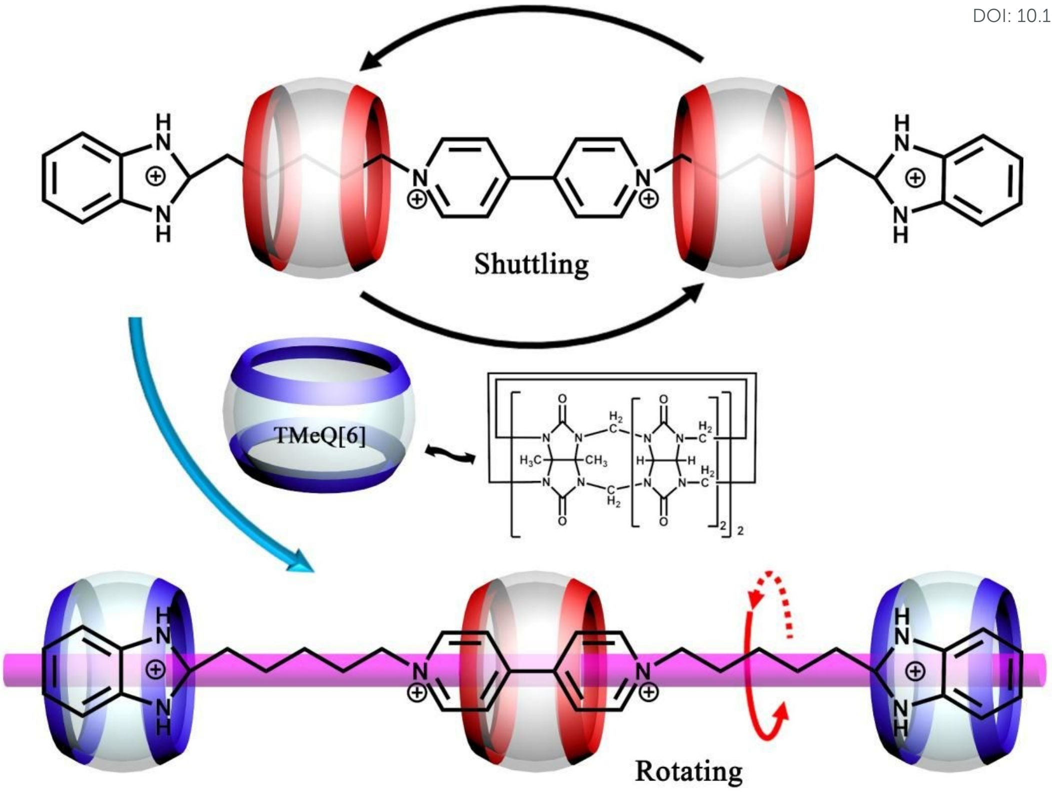

Figure 30 Schematic representation of the construction of a hetero[4]pseudorotaxane based on TMeQ[6] and Q[7].

6.3. Molecular encapsulation and release by substituted Q[*n*].

Artificial macrocyclic hosts have potential applications in various fields such as fragrance sustained-release, nutrient preservation, and drug delivery, molecular encapsulation and controlled release. Very recently, we have synthesized 1-(4-carboxybenzyl)-4 -[2-(4-pyridyl)-vinyl]-pyridinium chloride with *trans*- and *cis*-isomers.[153] The *trans*- and *cis*-form of the guest can be controlled by encapsulation and release by the molecular container TMeQ[6] under light irradiation and heating (Figure 31). The encapsulation of the *trans*-form into TMeQ[6] is attributed to strong host–guest interactions and hydrophobic effects while *cis*-form release from TMeQ[6] is attributed to a size effect.

View Article Online
DOI: 10.1039/D0QI00529K

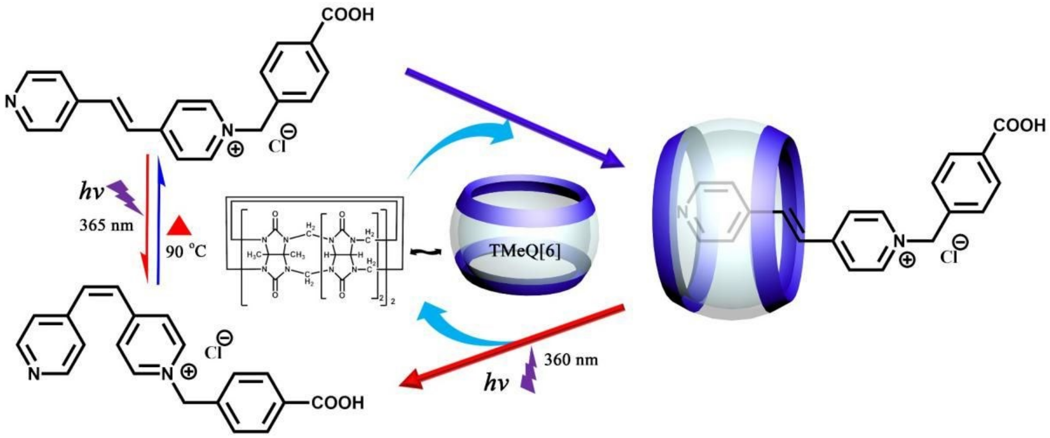

Figure 31 Guest encapsulation and release by TMeQ[6] under light irradiation and heating.

Very recently, we found another molecular encapsulation and release system based on $CyH_6Q[6]$ and 1,ω-bisbenzimidazolyl derivatives.[154] Experimental results revealed that all guests can form 1:1 or 1:2 inclusion complexes with $CyH_6Q[6]$ residing over benzoimidazole groups of the guests. Interestingly, the guest was released from the $CyH_6Q[6]$ cavity at high pH value and encapsulated back into the $CyH_6Q[6]$ cavity at low pH value.

6.4. Molecular switches

In 2017, we designed and successfully constructed an electrochemically-driven molecular switch involving a special axle guest hexyldimethyl(ferrocenylmethyl)ammonium bromide.[155] As shown in Figure 32, both hosts $CyH_6Q[6]$ and Q[7] can form different stable [2]pseudorotaxanes with the axle guest in its different redox states. Most importantly, the combination and dissociation of the hosts with the guest as well as the binding location can be controlled by electrochemical means.

View Article Online
DOI: 10.1039/D0QI00529K

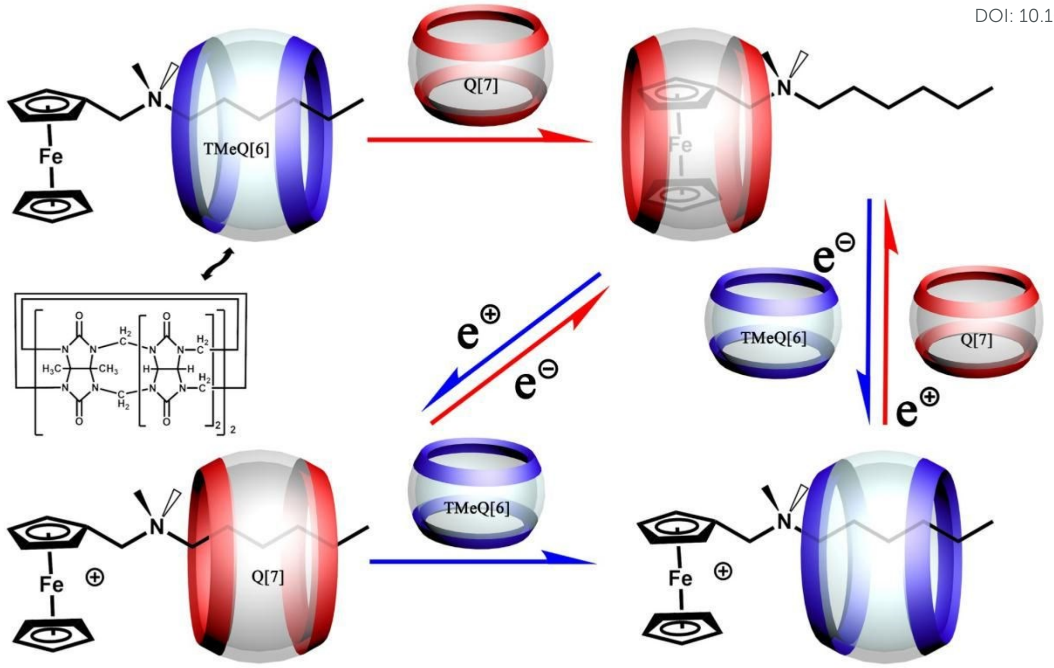

Figure 32 Electrochemically-driven molecular switch constructed by axle guest hexyldimethyl(ferrocenylmethyl)ammonium bromide with hosts $CyH_6Q[6]$ and Q[7].

7. Summary and Outlook

Almost two decades have passed since the first example of substituted Q[*n*] was reported by the Stoddart group. Numerous substituted Q[*n*]s have been designed and successfully synthesized, which addressed many long-standing concerns in cucurbituril chemistry. These substituted Q[*n*]s possess enhanced solubility in aqueous and organic media, good selectivity in molecular recognition, and high binding affinities to different metal ions. In particular, the synthesis of monohydroxylated Q[*n*]s provides an opportunity to further functionalize the substituted Q[*n*]s. In this review article, the recognition properties of the substituted Q[*n*]s toward many organic species have been demonstrated. The coordination structures and characteristics of substituted Q[*n*] with different metal ions, including alkali/alkaline-earth metals, transition metals, and lanthanides have also been identified. The supramolecular

View Article Online
DOI: 10.1039/D0QI00529K

properties of the substituted Q[*n*]s have led to their applications in areas as diverse as catalysis, sensors, hybrid materials, and gas inclusion and adsorption. The substituted Q[*n*]s also have been used in the construction of MIMs and molecular devices.

With the synthesis of more substituted Q[*n*]s, cucurbituril chemistry has ushered in a new era of development. The intrinsic properties of the substituted Q[*n*]s—high binding affinities, high selectivity, fine solubility in aqueous and organic media, diversity of cavity size and shape—suggest that substituted Q[*n*]s will become important components in MIMs. New molecular machines involving substituted Q[*n*]s with unprecedented characteristics are expected. The potential applications of substituted Q[*n*]s can be envisioned in pharmaceutical sciences, functional material science and beyond.

Acknowledgment

We thank the National Natural Science Foundation of China (Grant No.: 21371004 and 21601090), Natural Science Foundation of Anhui Province of China (1808085MB43, 2008085MB36), the Natural Science Foundation of Jiangsu Province (BK20160943) and the Priority Academic Program Development of Jiangsu Higher Education Institutions (PAPD) for financial support. CR thanks the EPSRC for financial support (Grant nos. EP/ L012804/1 and EP/ S025537/1).

DOI: 10.1039/D0QI00529K

References

[1] C. J. Pedersen, Cyclic polyethers and their complexes with metal salts, *J. Am. Chem. Soc.*, 1967, **89**, 2495–2496.

[2] C. J. Pedersen, Cyclic polyethers and their complexes with metal salts, *J. Am. Chem. Soc.*, 1967, **89**, 7017–7036.

[3] F. Diederich, *Cyclophanes*, The Royal Society of Chemistry, Cambridge, 1991.

[4] Z. Liu, S. K. M. Nalluri, J. F. Stoddart, Surveying macrocyclic chemistry: from flexible crown ethers to rigid cyclophanes. *Chem. Soc. Rev.*, 2017, **46**, 2459–2478.

[5] J. Murray, K. Kim, T. Ogoshi, W. Yao, B. C. Gibb, The aqueous supramolecular chemistry of cucurbit[*n*]urils, pillar[*n*]arenes and deep-cavity cavitands, *Chem. Soc. Rev.*, 2017, **46**, 2479–2496.

[6] M. J. Frampton, H. L. Anderson, Insulated molecular wires, *Angew. Chem., Int. Ed.*, 2007, **46**, 1028–1064.

[7] G. Yu, K. Jie, F. Huang, Supramolecular Amphiphiles Based on Host−Guest Molecular Recognition Motifs, *Chem. Rev.*, 2015, **115**, 7240–7303.

[8] L. Yang, X. Tan, Z. Wang, X. Zhang, Supramolecular Polymers: Historical Development, Preparation, Characterization, and Functions, *Chem. Rev.*, 2015, **115**, 7196–7239

[9] T. Ogoshi, T. Yamagishi, Pillar[5]- and pillar[6]arene-based supramolecular assemblies built by using their cavity-size-dependent host–guest interactions, *Chem. Commun.*, 2014, **50**, 4776–4787.

[10] O. A. Gerasko, D. G. Samsonenko, V. P. Fedin, Supramolecular chemistry of cucurbiturils, *Russ. Chem. Rev.*, 2002, **71**, 741–760.

[11] J. W. Lee, S. Samal, N. Selvapalam, H. J. Kim, K. Kim, Cucurbituril homologues and derivatives: new opportunities in supramolecular chemistry, *Acc. Chem. Res.*, 2003, **36**, 621–630.

[12] J. Lagona, P. Mukhopadhyay, S. Chakrabarti, L. Isaacs, The cucurbit[*n*]uril family, *Angew. Chem. Int. Ed.*, 2005, **44**, 4844–4870.

[13] E. Masson, X. X. Ling, R. Joseph, L. Kyeremeh-Mensah, X. Y. Lu, Cucurbituril chemistry: a tale of supramolecular success, *RSC Adv.*, 2012, **2**, 1213–1247.

[14] X. L. Ni, X. Xiao, H. Cong, L. L. Liang, K. Chen, X. J. Cheng, N. N. Ji, Q. J. Zhu, S. F. Xue, Z. Tao, Cucurbit[*n*]uril-based coordination chemistry: from simple coordination complexes to novel poly-dimensional coordination polymers, *Chem. Soc. Rev.*, 2013, **42**, 9480–9508.

[15] J. Lü, J. -X. Lin, M. -N. Cao, R. Cao, Cucurbituril: a promising organic building block for the design of coordination compounds and beyond, Coord. Chem. Rev., 2013, **257**, 1334–1356.

[16] A. E. Kaifer, Toward Reversible Control of Cucurbit[*n*]uril Complexes, *Acc. Chem. Res.*, 2014, **47**, 2160–2167.

[17] K. I. Assaf, W. M. Nau, Cucurbiturils: from synthesis to high-affinity binding and catalysis, *Chem. Soc. Rev.*, 2015, **44**, 394–418

[18] S. J. Barrow, S. Kasera, M. J. Rowland, J. Del. Barrio, O. A. Scherman, Cucurbituril-based molecular recognition, *Chem. Rev.*, 2015, **115**, 12320–12406.

[19] R. H. Gao, L. X. Chen, K. Chen, Z. Tao, X. Xiao, *Coord. Chem. Rev.*, 2017, **348**, 1–24.

[20] X. J. Cheng, L. L. Liang, K. Chen, N. N. Ji, X. Xiao, J. X. Zhang, Y. Q. Zhang, S. F. Xue, Q. J. Zhu, X. L. Ni, Z. Tao, Twisted cucurbit[14]uril, *Angew. Chem. Int. Ed.*, 2013, **52**, 7252–7255.

[21] R. Behrend, E. Meyer, F. Rusche, Condensation products of glycoluril and formaldehyde, *Liebigs Ann. Chem.*, 1905, **339**, 1–37.

[22] W. A. Freeman, W. L. Mock, N. -Y. Shih, Cucurbituril, *J. Am. Chem. Soc.*, 1981, **103**, 7367–7368.

[23] J. Kim, I. S. Jung, S. Y. Kim, E. Lee, J. K. Kang, S. Sakamoto, K. Yamaguchi, K. Kim, New cucurbituril homologues: syntheses, isolation, characterization, and X-ray crystal structures of cucurbit[*n*]uril (n = 5, 7, and 8), *J. Am. Chem. Soc.*, 2000, **122**, 540–541.

[24] A. I. Day, A. P. Arnold, R. J. Blanch, B. Snushall, Controlling factors in the synthesis of cucurbituril and its homologues, *J. Org. Chem.*, 2001, **66**, 8094–8100.

[25] H. J. Buschmann, R. C. Meschke, E. Schollmeyer, Complex formation of crown ethers and

cryptands with alkali metal and ammonium ions in chloroform, *J. Solution Chem.*, 2009, **38**, 209–217.

[26] W. Ong, A. E. Kaifer, Salt Effects on the Apparent Stability of the Cucurbit[7]uril-Methyl Viologen Inclusion Complex, *J. Org. Chem.*, 2004, **69**, 1383–1385.

[27] C. Márquez, R. R. Hudgins, W. M. Nau, Mechanism of Host−Guest Complexation by Cucurbituril, *J. Am. Chem. Soc.*, 2004, **126**, 5806–5816.

[28] Y. Kim, H. Kim, Y. H. Ko, N. Selvapalam, M. V. Rekharsky, Y. Inoue, K. Kim, Complexation of Aliphatic Ammonium Ions with a Water-Soluble Cucurbit[6]uril Derivative in Pure Water: Isothermal Calorimetric, NMR, and X-ray Crystallographic Study, *Chem. – Eur. J.*, 2009, **15**, 6143–6151.

[29] A. Flinn, G. C. Hough, J. F. Stoddart, D. J. Williams, Decamethylcucurbit[5]uril, *Angew. Chem. Int. Ed.*, 1992, **31**, 1475–1477.

[30] Y. Miyahara, K. Goto, M. Oka and T. Inazu, Remarkably Facile Ring-Size Control in Macrocyclization: Synthesis of Hemicucurbit[6]uril and Hemicucurbit[12]uril, *Angew. Chem., Int. Ed.*, 2004, **43**, 5019–5022.

[31] N. N. Andersen, M. Lisbjerg, K. Eriksen, M. Pittelkow, Hemicucurbit[*n*]urils and Their Derivatives-Synthesis and Applications, *Isr. J. Chem.*, 2018, **58**, 435–448

[32] M. Lisbjerg, B. M. Jessen, B. Rasmussen, B. E. Nielsen, A. Ø. Madsen, M. Pittelkow, Discovery of a cyclic 6 + 6 hexamer of D-biotin and formaldehyde, *Chem. Sci.*, 2014, **5**, 2647–2650.

[33] J. Svec, M. Necas, V. Sindelar, Bambus[6]uril, *Angew. Chem. Int. Ed.*, 2010, **49**, 2378-2381.

[34] C. A. Burnett, D. Witt, J. C. Fettinger, L. Isaacs, Acyclic Congener of Cucurbituril: Synthesis and Recognition Properties, *J. Org. Chem.*, 2003, **68**, 6184–6191.

[35] L. Gilberg, M. S. A. Khan, M. Enderesova, V. Sindelar, Cucurbiturils substituted on the methylene bridge, *Org. Lett.*, 2014, **16**, 2446–2449.

[36] J. Z. Zhao, H. J. Kim, J. Oh, S. Y. Kim, J. W. Lee, S. Sakamoto, K. Yamaguchi, K. Kim, Cucurbit[*n*]uril derivatives soluble in water and organic solvents, *Angew. Chem. Int. Ed.*, 2001,

View Article Online
DOI: 10.1039/D0QI00529K

40, 4233–4235.

[37] F. Wu, L.-H. Wu, X. Xiao, Y.-Q. Zhang, S. -F. Xue, Z. Tao, A. I. Day, Locating the Cyclopentano Cousins of the Cucurbit[*n*]uril Family, *J. Org. Chem.*, 2012, **77**, 606–611.

[38] Y. Zhao, V. Mandadapu, H. Iranmanesh, J. E. Beves, Anthony I. Day, The Inheritance Angle: A Determinant for the Number of Members in the Substituted Cucurbit[*n*]uril Family, *Org. Lett.*, 2017, **19**, 4034–4037.

[39] Y. J. Zhao, S. F. Xue, Q. J. Zhu, Z. Tao, J. X. Zhang, Z. B. Wei, L. S. Long, M. L. Hu, H. P. Xiao, A. I. Day, Synthesis of a symmetrical tetrasubstituted cucurbit[6]uril and its host−guest inclusion complex with 2,2’-bipyridine, *Chin. Sci. Bull.*, 2004, **49**, 1111–1116.

[40] J. J. Zhou, X. Yu, Y. C. Zhao, X. Xiao, Y. Q. Zhang, Q. J. Zhu, S. F. Xue, Q. J. Zhang, J. X. Liu, Z. Tao, Synthesis of a symmetrical octamethyl-substituted cucurbituril with a dimethyl-substituted glycoluril dimer, *Tetrahedron*, 2014, **70**, 800–804.

[41] J. J. Zhou, X. Yu, Y. C. Zhao, X. Xiao, Y. Q. Zhang, S. F. Xue, Z. Tao, J. X. Liu, Q. J. Zhu, Assemblies of alkaline-earth-metal ions with *o*-tetramethyl-substituted cucurbituril in the presence of the cadmium tetrachloride anion, *Eur. J. Inorg. Chem.*, 2014, **23**, 5771–5776.

[42] X. X. Wang, F. Y. Tian, M. Liu, K. Chen, Y. Q. Zhang, Q. J. Zhu, Z. Tao, A water soluble tetramethyl-substituted cucurbit[8]uril obtained from larger intermediates? *Tetrahedron*, 2019, **75**, 130488.

[43] J. X. Lin, Y. Q. Zhang, J. X. Zhang, S. F. Xue, Q. J. Zhu, Z. Tao, Synthesis of partially methyl substituted cucurbit[*n*]urils with 3a-methyl-glycoluril, *J. Mol. Struct.*, 2008, **875**, 442–446.

[44] C. Z. Wang, W. X. Zhao, Y. Q. Zhang, S. F. Xue, Q. J. Zhu, Z. Tao, A supramolecular assembly of methyl-substituted cucurbit[5]uril and its potential applications in selective absorption, *RSC Adv.*, 2015, **5**, 17354–17357.

[45] W. X. Zhao, C. Z. Wang, Y. Q. Zhang, S. F. Xue, Q. J. Zhu, Z. Tao, Supramolecular assembly of a methyl-substituted cucurbit[6]uril and its potential applications in selective sorption, *New J. Chem.*, 2015, **39**, 2433–2436.

[46] L. M. Zheng, J. N. Zhu, Y. Q. Zhang, Q. J. Zhu, S. F. Xue, Z. Tao, J. X. Zhang, Z. Xin, Z. B. Wei, L. S. Long, A. I. Day, Opposing substitution in cucurbit[6]urils forms ellipsoid cavities:

the symmetrical dicyclohexanocucurbit[6]uril is no exception highlighted by inclusion and exclusion complexes, *Supramol. Chem.*, 2008, **20**, 709–716.

[47] X. L. Ni, Y. Q. Zhang, Q. J. Zhu, S. F. Xue, Z. Tao, Crystal structures of host−guest complexes of meta-tricyclohexyl cucurbit[6]uril with small organic molecules, *J. Mol. Struct.*, 2008, **876**, 322–327.

[48] F. F. Shen, K. Chen, Y. Q. Zhang, Q. J. Zhu, Z. Tao, H. Cong, Mono- and dihydroxylated symmetrical octamethylcucurbiturils and allylated derivatives, *Org. Lett.*, 2016, **18**, 5544–5547.

[49] X. Yang, W. Zhao, Z. Wang, Y. Huang, S. M.Y. Lee, Z. Tao, R. Wang, Toxicity of hemimethyl-substituted cucurbit[7]uril, *Food and Chemical Toxicology*, 2017, **108**, 510–518.

[50] B. Vinciguerra, P. Y. Zavalij, L. Isaacs, Synthesis and Recognition Properties of Cucurbit[8]uril Derivatives, *Org. Lett.*, 2015, **17**, 5068–5071.

[51] S. Y. Jon, N. Selvapalam, D. H. Oh, J. K. Kang, S. Y. Kim, Y. J. Jeon, J. W. Lee, K. Kim, Facile synthesis of cucurbit[*n*]uril derivatives via direct functionalization: expanding utilization of cucurbit[*n*]uril, *J. Am. Chem. Soc.*, 2003, **125**, 10186–10187.

[52] S. K. Ghosh, A. Dhamija, Y. H. Ko, J. An, M. Y. Hur, D. R. Boraste, J. Seo, E. Lee, K. M. Park, K. Kim, Superacid-Mediated Functionalization of Hydroxylated Cucurbit[*n*]urils, *J. Am. Chem. Soc.*, 2019, **141**, 17503–17506.

[53] G. Sung, S.-Y. Lee, M.-G. Kang, K. L. Kim, J. An, J. Sim, S. Kim, S. Kim, J. Ko, H.-W. Rhee, K. M. Park, K. Kim, Supra-blot: an accurate and reliable assay for detecting target proteins with a synthetic host molecule–enzyme hybrid, *Chem. Commun.*, 2020, **56**, 1549–1552.

[54] N. Zhao, G. O. Lloyd, O. A. Scherman, Monofunctionalized cucurbit[6]uril synthesis using imidazolium host−guest complexation, *Chem. Commun.*, 2012, **48**, 3070–3072.

[55] B. Vinciguerra, L. Cao, J. R. Cannon, P. Y. Zavalij, C. Fenselau, L. Isaacs, Synthesis and self-assembly processes of monofunctionalized cucurbit[7]uril, *J. Am. Chem. Soc.*, 2012, **134**, 13133–13140.

[56] Y. Yu, J. Li, M. Zhang, L. Cao, L. Isaacs, Hydrophobic monofunctionalized cucurbit[7]uril undergoes self-inclusion complexation and forms vesicle-type assemblies, *Chem. Commun.*, 2015, **51**, 3762–3765.

[57] M. M. Ayhan, H. Karoui, M. Hardy, A. Rockenbauer, L. Charles, R. Rosas, K. Udachin, P. Tordo, D. Bardelang, O. Ouari, Comprehensive synthesis of monohydroxy-cucurbit[*n*]urils (*n* = 5, 6, 7, 8): high purity and high conversions, *J. Am. Chem. Soc.*, 2015, **137**, 10238–10245.

[58] M. M. Ayhan, H. Karoui, M. Hardy, A. Rockenbauer, L. Charles, R. Rosas, K. Udachin, P. Tordo, D. Bardelang, O. Ouari, Correction to "Comprehensive synthesis of monohydroxy-cucurbit[*n*]urils (*n* = 5, 6, 7, 8): high purity and high conversions", *J. Am. Chem. Soc.*, 2016, **138**, 2060–2061.

[59] N. Dong, J. He, T. Li, A. Peralta, M. R. Avei, M. Ma, A.E. Kaifer, Synthesis and Binding Properties of Monohydroxycucurbit[7]uril: A Key Derivative for the Functionalization of Cucurbituril Hosts, *J. Org. Chem.*, 2018, **83**, 5467–5473.

[60] L. Gilberg, M. S. A. Khan, M. Enderesova, V. Sindelar, Cucurbiturils Substituted on the Methylene Bridge, *Org. Lett.*, 2014, **16**, 2446–2449.

[61] J. Canceill, M. Cesario, A. Collet, J. Guilhem, C. Pascard, A New Bis-Cyclotribenzyl Cavitand Capable of Selective Inclusion of Neutral Molecules in Solution - Crystal-Structure of Its CH_2Cl_2 Cavitate, *J. Chem. Soc., Chem. Commun.*, 1985, **6**, 361–363.

[62] D. J. Cram, S. Karbach, Y. H. Kim, L. Baczynskyj, G. W. Kalleymeyn, Shell Closure of 2 Cavitands Forms Carcerand Complexes with Components of the Medium as Permanent Guests, *J. Am. Chem. Soc.*, 1985, **107**, 2575–2576.

[63] J. Rebek, Molecular behavior in small spaces, *Acc. Chem. Res.*, 2009, **42**, 1660–1668.

[64] D. Ajami, J. Rebek, More chemistry in small spaces, *Acc. Chem. Res.*, 2013, **46**, 990–999.

[65] B. Yang, L. M. Zheng, Z. Z. Gao, X. Xiao, Q. J. Zhu, S. F. Xue, Z. Tao, J. X. Liu, G. Wei, Extended and contorted conformations of alkanediammonium ions in symmetrical α,α',δ,δ'-tetramethyl-cucurbit[6]uril cavity, *J. Org. Chem.*, 2014, **79**, 11194–11198.

[66] C. L. Shan, B. Yang, W. Q. Sun, X. Xiao, Z. Tao, J. X. Liu, 1,3-propanediammonium and 1,12-dodecanediammonium encapsulated in the cavity of symmetrical α,α',δ,δ'-tetramethyl-cucurbit[6]uril, *Supramol. Chem.*, 2015, **27**, 606–612.

[67] G. S. Fang, W. Q. Sun, W. X. Zhao, R. L. Lin, Z. Tao, J. X. Liu, Host−guest complexation of di-cyclohexanocucurbit[6]uril and hexa-cyclohexano-cucurbit[6]uril with alkyldiammonium ions: A comparative study. *Org. Biomol. Chem.*, 2016, **14**, 674–679.

[68] Y. X. Qu, R. L. Lin, Y. Q. Zhang, K. Z. Zhou, Q. D. Zhou, Q. J. Zhu, Z. Tao, P. H. Ma, J. X. Liu, G. Wei, *Endo*/*exo* binding of alkyl and aryl diammonium ions by cyclopentanocucurbit[6]uril, *Org. Chem. Front.*, 2017, 4, 1799–1805.

[69] F. Biedermann, V. D. Uzunova, O. A. Scherman, W. M. Nau, A. D. Simone, Release of High-Energy Water as an Essential Driving Force for the High-Affinity Binding of Cucurbit[*n*]urils. *J. Am. Chem. Soc.*, 2012, 134, 15318–15323.

[70] L. J. Meng, X. Tian, S. Huang, R. L. Lin, X. H. Liu, Q. J. Zhu, Z. Tao, J. X. Liu, Solvent- and Heat-Dependent Binding Behaviors of HMeQ[6] with Alkyldiammonium Ions, *Chem. Select*, 2018, **3**, 9211–9217.

[71] W. X. Zhao, C. Z. Wang, L. X. Chen, X. W. Cui, R. L. Lin, Q. J. Zhu, Z. Tao, J. X. Liu, Host−guest complexation of HMeQ[7] with alkyldiammonium ions and alkyldiamines: A comparative study, *RSC Adv.*, 2016, **6**, 11937–11942.

[72] D. Lucas, T. Minami, G. Iannuzzi, L. Cao, J. B. Wittenberg, P. Anzenbacher, Jr., L. Isaacs, Templated Synthesis of Glycoluril Hexamer and Monofunctionalized Cucurbit[6]uril Derivatives, *J. Am. Chem. Soc.*, 2011, **133**, 17966–17976.

[73] L. Cao, L. Isaacs, Daisy Chain Assembly Formed from a Cucurbit[6]uril Derivative, *Org. Lett.*, 2012, **14**, 3072-3075.

[74] R. L. Lin, J. Q. Li, J. X. Liu, A. E. Kaifer, The Binding Interactions between Cyclohexanocucurbit[6]uril and Alkyl Viologens Give Rise to a Range of Diverse Structures in the Solid and the Solution Phases, *J. Org. Chem.*, 2015, **80**, 10505–10511.

[75] R. L. Lin, Y. P. Dong, Y. F. Hu, J. X. Liu, L. S. Bai, J. Y. Gao, H. L. Zhu, J. Zhao, Inclusion of methylviologen in symmetrical α,α’,δ,δ’-tetramethyl-cucurbit[6]uril, *RSC Adv.*, 2012, **2**, 7754–7758.

[76] H. Shi, L. M. Zheng, R. L. Lin, G. S. Fang, W. Q. Sun, J. X. Liu, Binding behaviors of *para*-dicyclohexanocucurbit[6]uril and *meta*-tricyclohexanocucurbit[6]uril with dialkyl viologens, *Supramol. Chem.*, 2018, **30**, 713–721.

[77] R. L. Lin, G. S. Fang, W. Q. Sun, J. X. Liu, Aniline-containing guests recognized by α,α’,δ,δ’-tetramethyl-cucurbit[6]uril host, *Sci. Rep.*, 2016, **6**, 39057.

[78] M. Qin, F. Y. Li, Y. Huang, W. Ran, D. Han, Y. L. Song, 20 Natural Amino Acids

Identification by a Photochromic Sensor Chip, *Anal. Chem.*, 2015, **87**, 837–842.

[79] Y. Zhou, J. Y. Yoon, Recent progress in fluorescent and colorimetric chemosensors for detection of amino acids, *Chem. Soc. Rev.*, 2012, **41**, 52–67.

[80] H. Heli, M. Hajjizadeh, A. Jabbari, A. A. Moosavi-Movahedi, Fine steps of electrocatalytic oxidation and sensitive detection of some amino acids on copper nanoparticles, *Anal. Biochem.*, 2009, **388**, 81–90.

[81] P. H. Shan, S. C. Tu, R. L. Lin, Z. Tao, J. X. Liu, X. Xiao, Supramolecular complexes of α,α’,δ,δ’-tetramethyl-cucurbit[6]uril binding with enantiomeric amino acids, *CrystEngComm*, 2017, **19**, 2168–2171.

[82] X. Xiao, Z. Z. Gao, C. L. Shan, Z. Tao, Q. J. Zhu, S. F. Xue, J. X. Liu, Encapsulation of haloalkane 1-(3-Chlorophenyl)-4-(3-chloropropyl)-piperazinium in symmetrical α,α’,δ,δ’-tetramethyl-cucurbit[6]uril, *Phys. Chem. Chem. Phys.*, 2015, **17**, 8618–8621.

[83] L. J. Meng, W. X. Zhao, L. X. Chen, W. Q. Sun, R. L. Lin, Q. J. Zhu, Z. Tao, J. X. Liu, Single and Double Binding of 1,10-Phenanthroline and 4,7-Dimethyl-1,10-phenanthroline to HMeQ[7]: Contrasting pKa Shifts Induced by HMeQ[7], *Chem. Select*, 2018, **3**, 1335–1341.

[84] Y. Fan, R. -H. Gao, X. Xiao, Z. Tao, Inclusion Complexes of Hymexazol with Three Different Cucurbit[*n*]uril: Preparation, and Physicochemical and Antifungal Characterization, *Isr. J. Chem.*, 2018, **58**, 466–471.

[85] Q. Liu, Q. Tang, Y. Y. Xi, Y. Huang, X. Xiao, Z. Tao, S. F. Xue, Q. J. Zhu, J. X. Zhang, G. Wei, *Supramol. Chem.*, 2015, **27**, 386–392

[86] H. Zhang, Y. Huang, S. F. Xue, Z. Tao, Q. J. Zhu, Host−guest interactions of 6-benzyladenine with normal and modified cucurbituril: ^{1}H NMR, UV absorption spectroscopy and phase solubility methods, *Supramol. Chem.*, 2011, **23**, 527–532.

[87] J. X. Liu, L. S. Long, R. B. Huang, L. S. Zheng, Molecular Capsules Based on Cucurbit[5]uril Encapsulating “Naked” Anion Chlorine, *Crystal Growth & Design.*, 2006, **6**, 2611–2614.

[88] X. Xiao, Z. Tao, Q. J. Zhu, S. F. Xue, J. X. Liu, G. Wei, Coordination Polymers Constructed from Alkali Metal Ions and $(HO)_{10}$cucurbit[5]uril, *CrystEngComm*, 2011, **13**, 3794–3800.

View Article Online
DOI: 10.1039/D0QI00529K

[89] X. L. Ni, J. X. Lin, Y. Y. Zheng, W. S. Wu, Y. Q. Zhang, S. F. Xue, Q. J. Zhu, Z. Tao, A. I. Day, Supramolecular bracelets and interlocking rings elaborated through the interrelationship of neighboring chemical environments of alkyl-substitution on cucurbit[5]uril, *Cryst. Growth Des.*, 2008, **8**, 3446–3450.

[90] Z. F. Li, F. Wu, F. G. Zhou, X. L. Ni, X. Feng, X. Xiao, Y. Q. Zhang, S. F. Xue, Q. J. Zhu, L. F. Lindoy, J. K. Clegg, Z. Tao, G. Wei, Approach to 10-Unit "Bracelet" Frameworks Based on Coordination of Alkyl-Substituted Cucurbit[5]urils and Potassium Ions, *Cryst. Growth Des.*, 2010, **10**, 5113–5116.

[91] Z. F. Li, L. L. Liang, F. Wu, F. G. Zhou, X. L. Ni, X. Feng, X. Xiao, Y. Q. Zhang, S. F. Xue, Q. J. Zhu, J. K. Clegg, Z. Tao, L. F. Lindoy, G. Wei, An approach to networks based on coordination of alkyl-substituted cucurbit[5]urils and potassium ions, *CrystEngComm*, 2013, **15**, 1994–2001.

[92] W.-J. Chen, L.-S. Long, R.-B. Huang, L.-S. Zheng, A Dihalide−Decahydrate Cluster of $[X_2(H_2O)_{10}]^{2-}$ in a Supramolecular Architecture of $\{[Na_2(H_2O)_6(H_2O@TMEQ[6])]\cdot 2(C_6H_5NO_3)\}X_2(H_2O)_{10}$ (TMEQ[6] = α,α′,δ,δ′-Tetramethylcucurbit[6]uril; X = Cl, Br), *Cryst. Growth Des.*, 2013, **13**, 2507−2513.

[93] J. Lin, J. Lü, M. Cao, R. Cao, Effects of Cocrystalline Subunits on the Supramolecular Chemistry of $Me_{10}Q[5]$: From Simple Inorganic Anions to Cluster Anions, *Cryst. Growth Des.*, 2011, **11**, 778–783.

[94] Y. -Q. Zhang, Q. -J. Zhu, S. -F. Xue, Z. Tao, Chlorine Anion Encapsulation by Molecular Capsules Based on Cucurbit[5]uril and Decamethylcucurbit[5]uril, *Molecules*, 2007, **12**, 1325–1333.

[95] Y. F. Hu, K. Chen, J. X. Liu, R. L. Lin, W. Q. Sun, Q. J. Zhu, S. F. Xue, Z. Tao, Complexation of Decamethylcucurbit[5]uril with Alkali Metal Ions, *Polyhedron*, 2012, **31**, 632–637.

[96] L. T. Wei, Y. Q. Zhang, K. Z. Zhou, L. L. Zhan, Y. X. Qu, Z. Tao, P. H. Ma, Coordination of fully substituted cyclopentano cucurbit[5]uril with alkali cation in the presence of tetrachloridezincate anion, *Inorg. Chim. Acta*, 2016, **445**, 1–7.

[97] F. F. Shen, J. L. Zhao, K. Chen, Z. Y. Hua, M. D. Chen, Y. Q. Zhang, Q. J. Zhu, Z. Tao, Supramolecular coordination assemblies of a symmetrical octamethyl-substituted cucurbituril

with alkali metal ions based on the outer-surface interactions of cucurbit[*n*]urils, *CrystEngComm*, 2017, **19**, 2464–2474.

[98] F. F. Shen, J. L. Zhao, K. Chen, J. Xu, Y. Wang, Z. Y. Hua, L. Wu, M. D. Chen, Y. Q. Zhang, Z. Tao, Coordination and supramolecular assemblies of mono-hydroxylated octamethylcucurbit[6]uril with alkali and alkaline earth metal ions in the presence of polychloride cadmium anions, *CrystEngComm*, 2017, **19**, 4017–4024.

[99] H. T. Hou, W. J. Chen, Y. Q. Zhang, Q. J. Zhu, S. F. Xue, Z. Tao, Coordination and supramolecular assemblies of meta-hexamethyl-substituted cucurbit[6]uril with alkali metal ions, *Polyhedron*, 2015, **87**, 117–121.

[100] X. L. Ni, X. Xiao, H. Cong, Q. J. Zhu, S. F. Xue, Z. Tao, Self-assemblies based on the "outer-surface interactions" of cucurbit[*n*]urils: new opportunities for supramolecular architectures and materials. *Acc. Chem. Res.*, 2014, **47**, 1386–1395.

[101] Y. Q. Zhang, L. M. Zhen, D. -H. Yu, Y. -J. Zhao, S. -F. Xue, Q. -J. Zhu, Z. Tao, Structures of supramolecular assemblies formed by substituted cucurbiturils and metal ions, *J. Mol. Struct.*, 2008, **875**, 435–441.

[102] Y. F. Hu, K. Chen, R. L. Lin, W. Q. Sun, J. Zhu, J. X. Liu, Q. J. Zhu, S. F. Xue, Z. Tao, Metal-ion-induced self-assembly of closed/opened molecular capsule based on pentacyclopentanocucurbit[5]uril, *RSC Adv.*, 2012, **2**, 5663–5668.

[103] L. T. Wei, Y. Q. Zhang, K. Z. Zhou, L. L. Zhan, Y. X. Qu, Z. Tao, P. H. Ma, Coordination of fully substituted cyclopentano cucurbit[5]uril with alkaline earth cations in the presence of tetrachlorozincate anions, *Inorg. Chim. Acta*, 2016, **453**, 277–283

[104] Y. X. Qu, Y. Q. Zhang, K. Z. Zhou, L. T. Wei, L. L. Zhan, S. Y. Cheng, Z. Tao, P. H. Ma, Interaction of Cyclopentano Cucurbit[6]uril with Alkaline Earth Cations and Supramolecular Assemblies with Aid of $[ZnCl_4]^{2-}$, *Chem. Select*, 2017, **2**, 4360–4363.

[105] C. Z. Wang, W. X. Zhao, F. F. Shen, Y. Q. Zhang, Q. J. Zhu, X. Xiao, Z. Tao, Methyl-substituted cucurbit[6]uril-based microporous supramolecular frameworks for highly selective Et_2O/CH_3OH adsorption, *CrystEngComm*, 2016, **18**, 2112–2118.

[106] R. H. Gao, Z. Y. Hua, K. Chen, J. Xu, Q. J. Zhu, Z. Tao, J. L. Zhao, Coordination supramolecular assemblies of a monohydroxycucurbit[7]uril and their potential applications in

DOI: 10.1039/D0QI00529K

gas sorption, *Dalton Trans.*, 2018, **47**, 1942–1947.

[107] J. X. Liu, C. H. Dong, L. S. Long, R. B. Huang, L. S. Zheng, From 1D zigzag chain to 1D tubular structure, weak field ligand-dependent assembly of cucurbit[6]uril-based tubular coordination polymer, *Dalton Trans.*, 2009, **36**, 7344–7346.

[108] X. Feng, Z. -F. Li, Z. Tao, S. -F. Xue, Q. -J. Zhu, Y. -Q. Zhang, J. X. Liu, Complexation of Cyclohexanocucurbit[6]uril with Cadmium Ions: X-ray Crystallographic and Electrochemical Study, *Inorg. Chem.*, 2010, **49**, 7638–7640.

[109] R. L. Lin, W. Q. Sun, W. R. Yao, J. Zhu, J. X. Liu, Anion Concentration Control in the Self-assembly of Symmetrical α,α’,δ,δ’-Tetramethyl-Cucurbit[6]uril-Based Tubular Architectures, *RSC Adv.*, 2014, **4**, 18323–18328.

[110] T. Zhang, Y. Q. Zhang, Q. J. Zhu, Z. Tao, Supramolecular assemblies based on the interaction of a copper dication with alky-substituted cucurbit[6]urils, *Polyhedron*, 2013, **53**, 98–102.

[111] W. W. Zhao, L. T. Wie, K. Z. Zhou, M. H. Chen, S. Y. Cheng, D. F. Jiang, P. H. Ma, A study on the coordination of fully substituted cyclopentano cucurbit[5, 6]uril with copper and zinc ions, *Chem. Select*, 2019, **4**, 11674–11677.

[112] A. Abdallah, S. Freslon, X. Fan, A. Rojo, C. Daiguebonne, Y. Suffren, K. Bernot, G. Calvez, T. Roisnel and O. Guillou, Lanthanide-Based Coordination Polymers With 1,4-Carboxyphenylboronic Ligand: Multiemissive Compounds for Multisensitive Luminescent Thermometric Probes, *Inorg. Chem.*, 2019, **58**, 462–475.

[113] Y. Cui, J. Zhang, H. He and G. Qian, Photonic functional metal-organic frameworks, *Chem. Soc. Rev.*, 2018, **47**, 5740–5785.

[114] Y. Cui, B. Li, H. He, W. Zhou, B. Chen and G. Qian, Metal-Organic Frameworks as Platforms for Functional Materials, *Acc. Chem. Res.*, 2016, **49**, 483–493.

[115] J. X. Liu, Y. F. Hu, R. L. Lin, W. Q. Sun, X. F. Chu, Q. J. Zhu, S. F. Xue, Z. Tao, Coordination Complexes Based on Pentacyclohexanocucurbit[5]uril and Lanthanide(III) Ions: Lanthanide Contraction Effect Induced Structural Variation, *CrystEngComm*, 2012, **14**, 6983–6989.

[116] X. Qin, X. L. Ni, J. X. Hu, K. Chen, Y. Q. Zhang, C. Redshaw, Q. J. Zhu, S. F. Xue, Z.

Tao, Macrocycle-based metal ion complexation: a study of the lanthanide contraction effect towards hexacyclohexanocucurbit[6]uil, *CrystEngComm*, 2013, **15**, 738–744.

[117] C. Z. Wang, W. X. Zhao, Y. Q. Zhang, S. F. Xue, Z. Tao, Q. J. Zhu, Interaction of Ln^{3+} with Methyl-Substituted Cucurbit[*n*]urils (*n* = 5, 6) Derived from 3a-Methyl Glycoluril, *ChemPlusChem*, 2015, **80**, 1052–1059.

[118] X. Yu, J. K. Clegg, Y. Q. Zhang, S. F. Xue, Z. Tao, Q. J. Zhu, L. F. Lindoy, G. Wei, Adducts of aqua complexes of Ln^{3+} with ortho-tetramethyl substituted cucurbituril: Potential applications for isolation of heavier lanthanides, *Polyhedron*, 2015, **91**, 150–154.

[119] R. L. Lin, J. J. Zhou, F. H. Zhou, W. Q. Sun, J. X. Liu, K. Chen, Lanthanide contraction effect and organic additive impact the coordination structures of lanthanide ions with symmetrical octamethyl-substituted cucurbit[6]uril ligand, *CrystEngComm*, 2019, **21**, 5641–5649.

[120] Y. X. Qu, K. Z. Zhou, K. Chen, Y. Q. Zhang, X. Xiao, Q. D. Zhou, Z. Tao, P. H. Ma, G. Wei, Coordination and Supramolecular Assemblies of Fully Substituted Cyclopentanocucurbit[6]uril with Lanthanide Cations in the Presence of Tetrachlorozincate Anions, and Their Potential Applications, *Inorg. Chem.*, 2018, **57**, 7412–7419.

[121] F. F. Shen, K. Chen, Z. Y. Hua, Y. Wang, J. Xu, M. D. Chen, Y. Q. Zhang, Z. Tao, Adducts of aqua complexes of Ln^{3+} with a dihydroxylated symmetrical octamethyl-substituted cucurbituril: potential applications for isolation of heavier lanthanides, *CrystEngComm*, 2017, **19**, 5635–5639.

[122] J. J. Zhou, X. Yu, Y. C. Zhao, X. Xiao, Y. Q. Zhang, Q. J. Zhu, S. F. Xue, Z. Tao, J. X. Liu, Q. J. Zhu, Coordination of Ln^{3+} in *ortho*-tetramethyl-substituted cucurbituril supramolecular assemblies formed in the presence of nitrate cadmium: potential applications for isolation of heavier lanthanides, *CrystEngComm*, 2014, **16**, 10674–10680.

[123] L. M. Zheng, J. X. Liu, Lanthanide Contraction Effect on Crystal Structures of Lanthanide Coordination Polymers with Cyclohexanocucurbit[6]uril Ligand. *J. Solid State Chem.*, 2017, **245**, 45–49.

[124] H. F. Li, J. Lü, J. X. Lin, Y. Huang, M. Cao, R. Cao, Crystalline Hybrid Solid Materials of Palladium and Decamethylcucurbit[5]uril as Recoverable Precatalysts for Heck Cross-Coupling Reactions, *Chem. – Eur. J.*, 2013, **19**, 15661–15668.

[125] H. F. Li, J. Lü, J. X. Lin, R. Cao, Monodispersed Ag Nanoparticles as Catalyst: Preparation Based on Crystalline Supramolecular Hybrid of Decamethylcucurbit[5]uril and Silver Ions, *Inorg. Chem.*, 2014, **53**, 5692–5697.

[126] M. T. Pope, A. Müller, Polyoxometalates: From Platonic Solids to Antiviral Activity, Kluwer, Dordrecht, The Netherlands, 1994.

[127] X. K. Fang, P. Kogerler, L. Isaacs, S. Uchida, N. Mizuno, Cucurbit[*n*]uril -polyoxoanion hybrids. *J. Am. Chem. Soc.*, 2009, **131**, 432–433.

[128] J. X. Lin, J. Lü, R. Cao, J. T. Chen, C. Y. Su, Supramolecular assembly from decavanadate anion and decamethylcucurbit[5]uril. *Dalton Trans.*, 2009, **38**, 1101–1103.

[129] J. X. Lin, J. Lü, H. X. Yang, R. Cao, Construction of train-like supramolecular structures from decamethylcucurbit[5]uril and iso- or Hetero-Keggin-Type polyoxotungstates. *Cryst. Growth Des.*, 2010, **10**, 1966–1970.

[130] J. X. Lin, J. Lü, M. N. Cao, R. Cao, Effects of cocrystalline subunits on the supramolecular chemistry of $Me_{10}Q[5]$: from simple inorganic anions to cluster anions. *Cryst. Growth Des.*, 2011, **11**, 778–783.

[131] L. W. Han, J. Lü, J. X. Lin, R. Cao, New types of hybrid solids of tetravanadate polyanions and cucurbituril. *Dalton Trans.*, 2012, **41**, 10080–10084.

[132] M. Cao, J. X. Lin, J. Lü, Y. You, T. Liu, R. Cao, Development of a polyoxometallate-based photocatalyst assembled with cucurbit[6]uril via hydrogen bonds for azo dyes degradation. *J. Hazard. Mater.*, 2011, **186**, 948–951.

[133] J. Lü, J. X. Lin, X. L. Zhao, R. Cao, Photochromic hybrid materials of cucurbituril and polyoxometalates as photocatalysts under visible light. *Chem. Commun.*, 2012, **48**, 669–671.

[134] B. X. Han, C. Z. Wang, Y. Zhao, K. Chen, X. Xiao, Q. J. Zhu, S. F. Xue, Y. Q. Zhang, Z. Tao, $[PMo_{12}O_{40}]^{3-}$-induced perhydroxycucurbit[5]uril-based porous supramolecular assemblies. *Eur. J. Inorg. Chem.*, 2014, **23**, 831–835.

[135] B. X. Han, C. Z. Wang, K. Chen, X. Xiao, Z. Tao, S. F. Xue, Y. Q. Zhang, Q. J. Zhu, Coordination and supramolecular assemblies of K^+/Ln^{3+} to perhydroxycucurbit[5]uril in the presence of $[PMo_{12}O_{40}]^{3-}$: potential application in isolation of light lanthanides. *CrystEngComm*, 2014, **16**, 1615–1619.

[136] L. W. Han, J. X. Lin, Q. Yin, B. Karadeniz, H. F. Li, J. Lü, R. Cao, Sandwich-type Inorganic−Organic Hybrid Solids of Iso-polyvanadate Clusters and Decamethylcucurbit[5]uril, *Cryst. Growth Des.*, 2016, **16**, 1213–1217.

[137] X. Xia, W. W. Ge, H. Chen, Z. Tao, Y. Zhang, G. Wei, K. Chen, Porous supramolecular assemblies and functional properties of perhydroxylated cucurbit[6]uril and polyoxometallates, *New J. Chem.*, 2019, **43**, 10297–10304.

[138] Q. Bai, S. Zhang, H. Chen, T. Sun, C. Redshaw, J. X. Zhang, X. L. Ni, G. Wei, Z. Tao, Alkyl Substituted Cucurbit[6]uril Assisted Competitive Fluorescence Recognition of Lysine and Methionine in Aqueous Solution, *Chem. Select.,* 2017, **2**, 2569–2573.

[139] A. T. Bockus, L. C. Smith, A. G. Grice, O. A. Ali, C. C. Young, W. Mobley, A. Leek, J. L. Roberts, B. Vinciguerra, L. Isaacs, A. R. Urbach, Cucurbit[7]uril−Tetramethylrhodamine Conjugate for Direct Sensing and Cellular Imaging, *J. Am. Chem. Soc.*, 2016, **138**, 16549–16552.

[140] N. H. Kim, W. Hwang, K. Baek, M. R. Rohman, J. Kim, H. W. Kim, J. Mun, S. Y. Lee, G. Yun, J. Murray, J. W. Ha, J. Rho, M. Moskovits, and K. Kim, Smart SERS Hot Spots: Single Molecules Can Be Positioned in a Plasmonic Nanojunction Using Host−Guest Chemistry, *J. Am. Chem. Soc.*, 2018, **140**, 4705–4711.

[141] G. Huber, P. Berthault, A. L. Nguyen, A. Pruvost, E. Barruet, J. Rivollier, M. P. Heck, B. Prieur, Cucurbit[5]uril derivatives as oxygen carriers, *Supramol. Chem.*, 2019, **31**, 668–675.

[142] M. Zhang, H. Shi, D. Meng, K. Chen, Lin, R. L. W.Q. Sun, J. X. Liu, Encapsulation and removal of aniline by di-cyclohexanocucurbit[6]uril, *New J. Chem.*, 2019, **43**, 1487–1493.

[143] C. Z. Wang, W. X. Zhao, Y. Q. Zhang, S. F. Xue, Q. J. Zhu, Z. Tao, A supramolecular assembly of methyl-substituted cucurbit[5]uril and its potential applications in selective absorption, *RSC Adv.*, 2015, **5**, 17354–17357.

[144] W. X. Zhao, C. Z. Wang, Y. Q. Zhang, S. F. Xue, Q. J. Zhu, Z. Tao, Supramolecular assembly of a methyl-substituted cucurbit[6]uril and its potential applications in selective sorption, *New J. Chem.*, 2015, **39**, 2433–2436.

[145] X. Xia, K. Chen, Y. Q. Yao, C. Y. Shan, Z. Tao, Y. Q. Zhang, Q. D. Zhou, G. Wei, Highly selective absorption of polychloromethanes in perhydroxylated cucurbit[6]uril-based

View Article Online
DOI: 10.1039/D0QI00529K

supramolecular assemblies, *New J. Chem.*, 2018, **42**, 802–806.

[146] K. M. Park, D. Whang, E. Lee, J. Heo, K. Kim, Transition Metal Ion Directed Supramolecular Assembly of One and Two-Dimensional Polyrotaxanes Incorporating Cucurbituril, *Chem. – Eur. J.*, 2002, **8**, 498–508.

[147] L. He, J. P. Zeng, D. H. Yu, H. Cong, Y. Q. Zhang, Q. J. Zhu, S. F. Xue, Z. Tao, Kinetic and thermodynamic inclusion complexes of symmetric tetramethyl-substituted cucurbit[6]uril with HCl salts of *N*,*N*′-bis(pyridylmethyl)-1,6-hexanediamine, *Supramol. Chem.*, 2010, **22**, 619–628.

[148] J. P. Zeng, H. Cong, K. Chen, Z. Tao, S. F. Xue, Q. J. Zhu, Y. Q. Zhang, J. X. Liu, Novel Strategy to Assemble Achiral Ligands to Chiral Helical Polyrotaxanes Structures, *Inorg. Chem.*, 2011, **50**, 6521–6525.

[149] X. Wei, J. P. Zeng, H. Cong, Y. Q. Zhang, Z. Tao, Q. J. Zhu, S. F. Xue, Synthesis of supramolecular polyrotaxanes assemblies incorporating symmetrical α,α′,δ,δ′-tetramethyl-cucurbit[6]uril moieties using polychloride zinc(II) and cadmium(II) anions, *Supramol. Chem.*, 2014, **26**, 692–697.

[150] Z. Xiao, R. L. Lin, Q. Y. Liu, Z. Tao, J. X. Liu, X. Xiao, Multiple noncovalent interactions constructed polymeric supramolecular crystals: recognition of butyl viologen by para-dicyclohexano cucurbit[6]uril and α,α’,δ,δ’-tetramethylcucurbit[6]uril, *Org. Chem. Front.*, 2017, **4**, 2422–2427.

[151] W. J. Wu, F. Wu, A. I. Day, Molecular Snuggle and Stretch of a Tetraammonium Chain in the Construction of a Hetero-[4]pseudorotaxane with CyclopentanoQ[6] and Classical Q[7]. *J. Org. Chem.*, 2017, **82**, 5507–5515.

[152] R. L. Lin, R. Li, H. Shi, K. Zhang, D. Meng, W. Q. Sun, K. Chen, J. X. Liu, Symmetrical-Tetramethyl-Cucurbit[6]uril-Driven Movement of Cucurbit[7]uril Gives Rise to Heterowheel [4]Pseudorotaxanes, *J. Org. Chem.*, 2020, **85**, 3568–3575.

[153] K. Zhang, W. Q. Sun, R. L. Lin, X. Xiao, Z. Tao, J. X. Liu, Controlled encapsulation and release of an organic guest in the cavity of α,α’,δ,δ’-tetramethylcucurbit[6]uril, *Eur. J. Org. Chem.*, 2019, **7**, 1503–1507.

[154] L. M. Zheng, K. Zhang, R. L. Lin, X.F. Chu, J. X. Liu, Binding interactions of

View Article Online
DOI: 10.1039/D0QI00529K

bisbenzimidazolyl derivatives with cyclohexanocucurbit[6]uril, *J. Incl. Phenom. Macrocycl. Chem.*, 2020, **96**, 125–135.

[155] H. Shi, W. Q. Sun, R. L. Lin, C. H. Liu, J. X. Liu, Construction of a molecular switch and selector under electrochemical control, *ACS Omega*, 2017, **2**, 4575–4580.

Table 1 Synthesis of substituted Q[*n*]s

No.	Synthetic Strategy	Yields	Refs
1	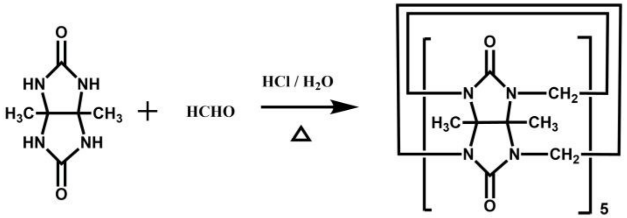	Me$_{10}$Q[5]: 16%	[29]
2	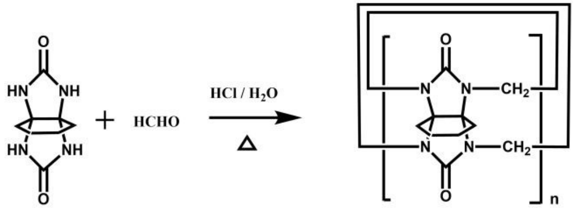	CyH$_5$Q[5]: 16% CyH$_6$Q[6]: 2%	[36]
3	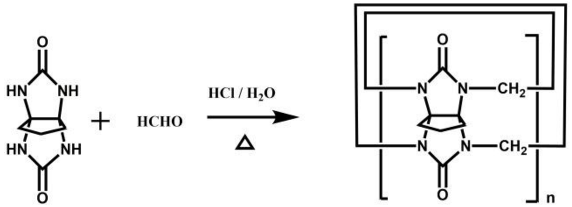	CyP$_5$Q[5]: 3.2% CyP$_6$Q[6]: 5.2% CyP$_7$Q[7]: 1.4%	[37]
4	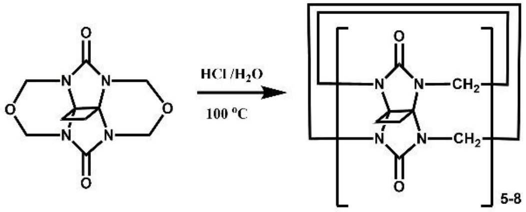	CyB$_5$Q[5]: 10% CyB$_6$Q[6]: 13% CyB$_7$Q[7]: 4% CyB$_8$Q[8]: 1%	[38]

5	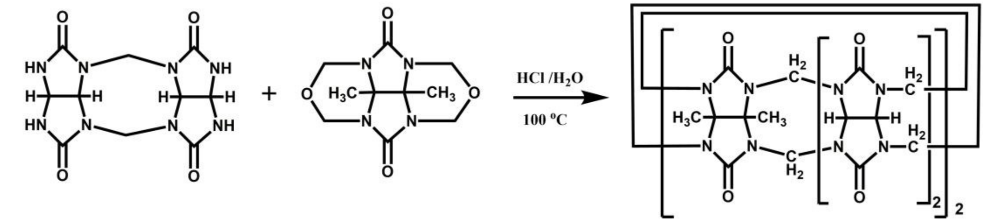	TMeQ[6]: 30%	[39]
6	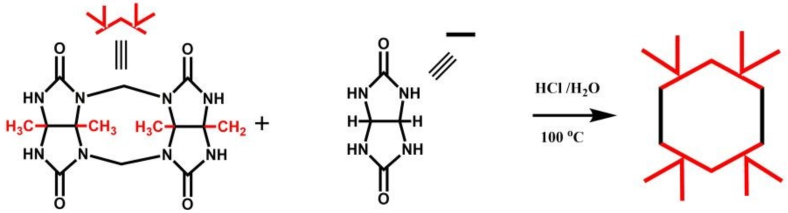	OMeQ[6]: 3.4%	[40]
7	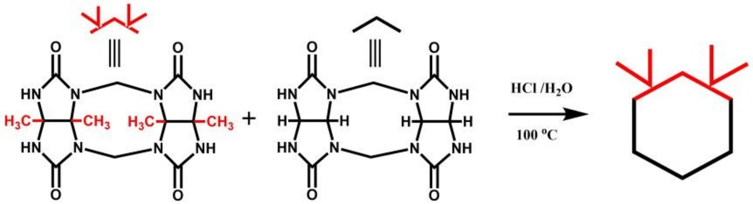	*o*-TMeQ[6]: 3.4%	[41]
8	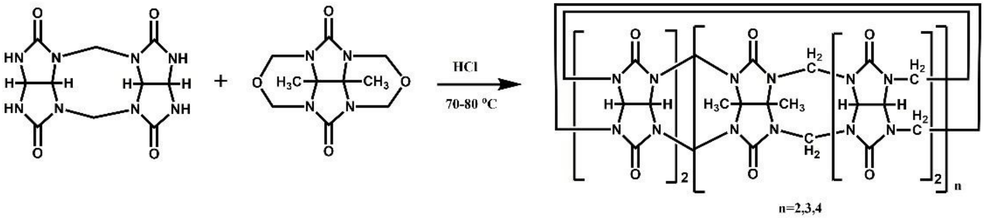	*m*-Me$_4$Q[8]: 4%	[42]

9	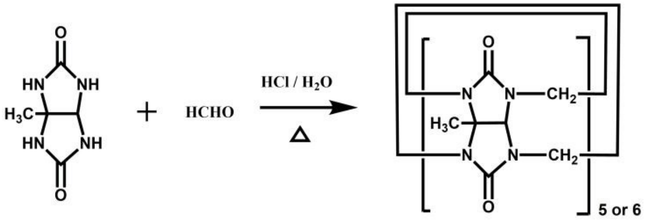	$\mathrm{HMe_5Q[5]}$: 6.4% $\mathrm{HMe_6Q[6]}$: 5.8%	[43]
10	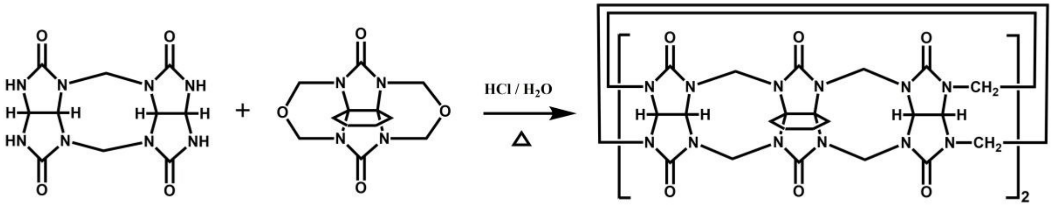	$\mathrm{CyH_2Q[6]}$: 30%	[46]
11	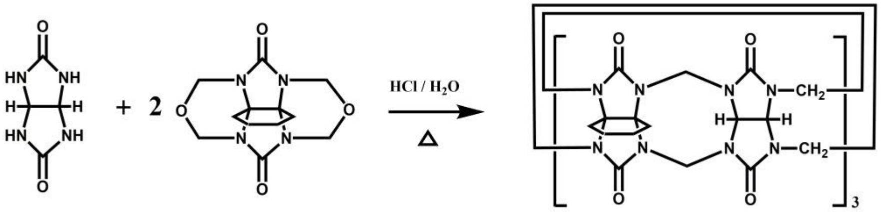	$\mathrm{CyH_3Q[6]}$: 39.6%	[47]
12	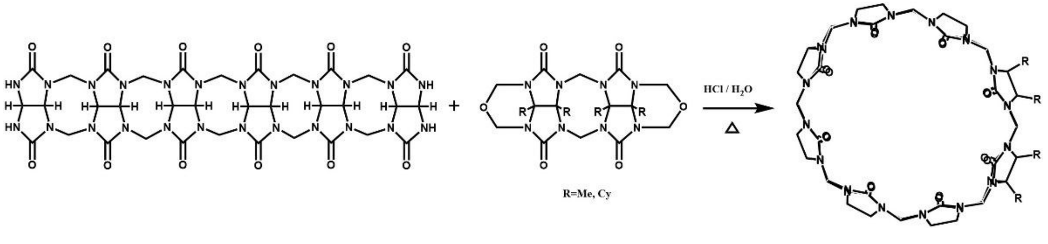	*o*-$\mathrm{Me_4Q[8]}$: 11% *o*-$\mathrm{CyH_2Q[8]}$: 4%	[50]

13	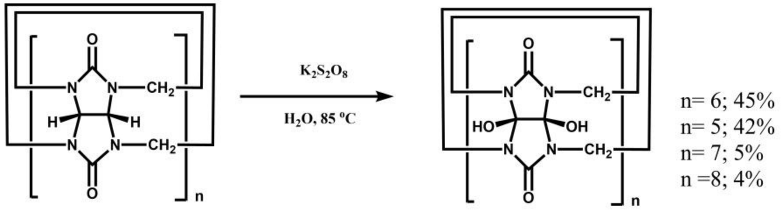	(HO)$_{10}$Q[5]: 42% (HO)$_{12}$Q[6]: 45% (HO)$_{14}$Q[7]: 5% (HO)$_{16}$Q[8]: 4%	[51]
14	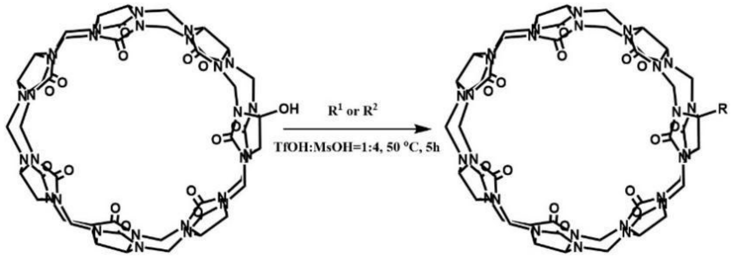	Q[7]-NHCO-CH$_2$CH$_3$: 96% Q[7]-NHCO-CHCH$_2$: 87% Q[7]-NHCO-CH$_2$CN: 94% Q[7]-NHCO-CH$_2$CO$_2$H: 84% Q[7]-NHCO-C$_6$H$_5$: 63% Q[7]-NHCO-(CH$_2$)$_2$Br: 73% Q[7]-O-(CH$_2$)$_3$OH: 76% Q[7]-O-(CH$_2$)$_3$Br: 63%	[52]
15	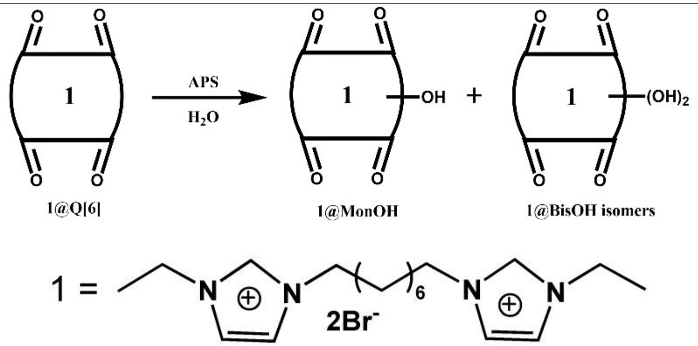	(HO)$_1$Q[6]: 12%	[54]

16	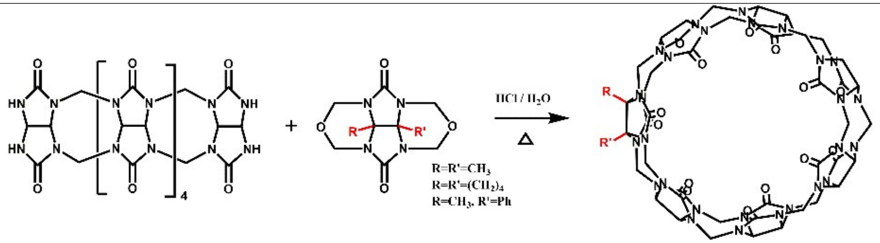	Me$_2$Q[7]: 31% CyHQ[7]: 18% MePhQ[7]: 3%	[55]
17	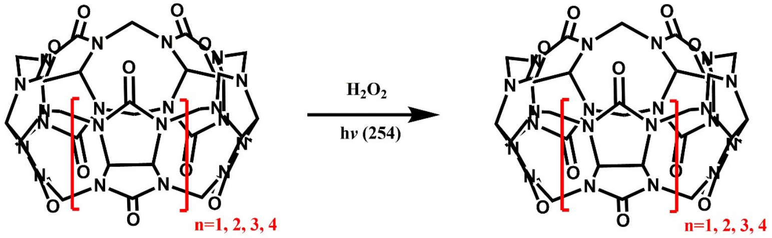	(HO)$_1$Q[5]: 95% (HO)$_1$Q[6,7]: 95-100% (HO)$_1$Q[8]: 90%	[57]
18	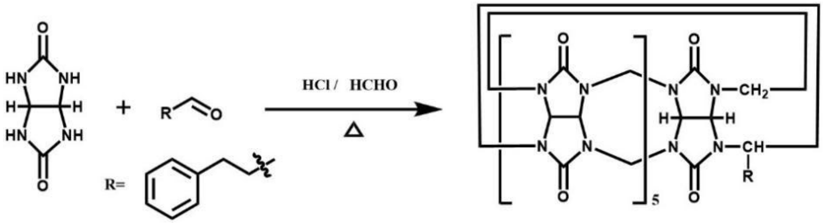	PheQ[6]: 0.2%	[60]

Table 2 A list of the substituted Q[*n*]-based coordination compounds. For the sake of clarity, they are named according to the type of the metal ions contained in the compounds: A for alkali metal, AE for alkali-earth metal, TM for transition metal, and Ln for lanthanide metals.

Compounds	Formula	Structural type	Ref.
A-1	$\{[K(H_2O)](NO_3@(HO)_{10}Q[5])[K(\mu\text{-}NO_3)]\}Cl(H_3O)_2^{2+}\cdot 7H_2O$	2-D	[88]
A-2	$\{[Rb_3(\mu_2\text{-}H_2O)(\mu_3\text{-}H_2O)(H_2O)_5SO_4]^+(H_2O@(HO)_{10}Q[5])\}Cl(H_3O)^+\cdot 2H_2O$	1-D	[88]
A-3	$[Cs_2(H_2O@(HO)_{10}Q[5])]SO_4^{2-}(H_3O)_4^{4+}$	2-D	[88]
A-4	$\{Sr_2(Cl@Me_2Q[5]\}3Cl\cdot 19H_2O$	2-D	[89]
A-5	$\{K_2(H_2O@1,2,4\text{-}CyH_3Q[5])\}2Cl\cdot 15.5H2O.$	3-D	[89]
A-6	$\{[K_2(1,2,4\text{-}Me_6Q[5])]_3(H_2O)_4\}^{6+}\cdot 6Cl^-\cdot 47(H_2O)$	3-D	[90]
A-7	$\{[K_2(CyH_5Q[5])]_34(H_2O)\}^{6+}\cdot 6I^-\cdot 23(H_2O)$	3-D	[91]
A-8	$\{K_6(H_2O)_4[H_2O@Me_2Q[5]]_3\}\cdot 6I\cdot 39H_2O$	2-D	[91]
A-9	$\{K_6(H_2O)_4[H_2O@1,3\text{-}CyH_2Q[5]]_2[H_2O@1,2,4\text{-}CyH_3Q[5]]\}\cdot 6I\cdot 46H_2O$	2-D	[91]
A-10	$\{K_6(H_2O)_4[H_2O@1,2,4\text{-}CyH_3Q[5]]_3\}\cdot 6Cl\cdot 55H_2O$	2-D	[91]
A-11	$\{K_6(H_2O)_4[H_2O@1,2,3\text{-}CyH_3Q[5]]_3\}\cdot 6I\cdot 26H_2O$	2-D	[91]
A-12	$\{K_6(H_2O)_4[H_2O@CyH_5Q[5]]_3\}\cdot 6Cl\cdot 53H_2O$	2-D	[91]
A-13	$\{[Na_2(H_2O)_6(H_2O@TMeQ[6])]\cdot 2(C_6H_5NO_3)\cdot Cl_2(H_2O)_{10}\}$	1-D	[92]

A-14	$\{[Na_2(H_2O)_6(H_2O@TMeQ[6])]\cdot 2(C_6H_5NO_3)\cdot Br_2(H_2O)_{10}\}$	1-D	[92]
A-15	$\{[Na_2(H_2O)_6(C_6H_5NO_3)_2(2H_2O@TMeQ[6])]\cdot 6(C_6H_5NO_3)\}F_2(H_2O)_4\}$	1-D	[92]
A-16	$[K_2(H_2O)_3((H_2O)_{0.5}@Me_{10}Q[5])]\cdot Cl_2$	1-D	[93]
A-17	$[K_2(H_2O)_2(H_2O@Me_{10}Q[5])]\cdot(ClO_4)_2\cdot 3H_2O$	0-D	[93]
A-18	$[K_2(H_2O)_2(SCN)(Me_{10}Q[5])]\cdot(SCN)\cdot H_2O$	0-D	[93]
A-19	$[Sr_2Me_{10}Q[5](H_2O)_4Cl]^{3+}\cdot 3Cl^{-}\cdot 2(HCl)\ \cdot 19H_2O$	0-D	[94]
A-20	$[K(H_2O)Me_{10}Q[5]Cl]\cdot[Zn(H_2O)_2Cl_2]\cdot[ZnCl_4]^{2-}\cdot 2(H_3O)^{+}\cdot 8H_2O$	0-D	[94]
A-21	$[Na(H_2O)(H_2O)_2@Me_{10}Q[5]](C_6H_6O_2)_2Cl\cdot 8H_2O$	0-D	[95]
A-22	$[K_2(H_2O)_2(H_2O)@Me_{10}Q[5]](C_6H_6O_2)_2Cl_2\cdot 7H_2O$	1-D	[95]
A-23	$[Rb_2(H_2O)_2(H_2O)@Me_{10}Q[5]](C_6H_6O_2)_2Cl_2\cdot 7H_2O$	1-D	[95]
A-24	$[Cs(H_2O)_2(H_2O@Me_{10}Q[5]](C_6H_6O_2)_2Cl\cdot 6H_2O$	0-D	[95]
A-25	$\{Na_2(H_2O)_2Cl@CyP_5Q[5]\}\cdot[ZnCl_4]\cdot H_3O\cdot 9H_2O$	0-D	[96]
A-26	$\{K_2(H_2O)_2Cl@CyP_5Q[5]\}\cdot[ZnCl_4]\cdot H_3O\cdot 10H_2O$	0-D	[96]
A-27	$\{Rb_2CyP_5Q[5]\}\cdot[ZnCl_4]\cdot 3H_2O$	0-D	[96]
A-28	$\{Cs_2CyP_5Q[5]\}\cdot[ZnCl_4]\cdot 3H_2O$	1-D	[96]
A-29	$OMeQ[6]\cdot[Cd_2Cl_7]\cdot 3H_3O\cdot 10H_2O$	0-D	[97]

A-30	$\{K_4(H_2O)_{10}OMeQ[6]\}\cdot[Cd_2Cl_8]\cdot 2H_2O$	1-D	[97]
A-31	$OMeQ[6]\cdot[CdCl_4]\cdot 2H_3O\cdot 11H_2O$	0-D	[97]
A-32	$\{CsOMeQ[6]\}\cdot[Cd_2Cl_7]\cdot 2H_3O\cdot 5H_2O$	0-D	[97]
A-33	$\{Na_2(H_2O)_6(p\text{-Hyb})_2OMeQ[6]\}\cdot 2(p\text{-Hyb})\cdot 2Cl\cdot H_2O$	0-D	[97]
A-34	$\{Cs(H_2O)OMeQ[6]\}\cdot 4(p\text{-Hyb})\cdot 3H_3O\cdot 7H_2O$	0-D	[97]
A-35	$\{Na_2(H_2O)_{10}(HO)_1OMeQ[6]\}\cdot 2[CdCl_4]\cdot 2H_3O\cdot 3H_2O$	0-D	[98]
A-36	$\{K_2(H_2O)_{10}(HO)_1OMeQ[6]\}\cdot 2[CdCl_4]\cdot 2H_3O\cdot 2H_2O$	1-D	[98]
A-37	$\{Rb(H_2O)_8(HO)_1OMeQ[6]\}\cdot 2[CdCl_4]\cdot 3H_3O\cdot H_2O$	1-D	[98]
A-38	$\{K_2(H_2O)_6(1,3,5\text{-}Me_6Q[6])\}^{2+}\cdot Cr_2O_7{}^{2-}\cdot 15H_2O$	0-D	[99]
A-39	$\{Rb_2(H_2O)_6(1,3,5\text{-}Me_6Q[6])\}^{2+}\cdot 2Cl^{-}\cdot 14H_2O$	0-D	[99]
A-40	$\{Cs_2(H_2O)_6(1,3,5\text{-}Me_6Q[6])\}^{2+}\cdot 2Cl^{-}\cdot 11H_2O$	1-D	[99]
A-41	$[Li_2(H_2O)_4\{H_2O@Me_{10}Q[5]\}\cdot PdCl_4\cdot 4H_2O$	0-D	[124]
A-42	$[Na_2(H_2O)_5\{H_2O@Me_{10}Q[5]\}\cdot PdCl_4\cdot 5H_2O$	0-D	[124]
A-43	$[K_2(H_2O)_3\{(H_2O)_{0.5}@Me_{10}Q[5]\}]\cdot PdCl_4$	2-D	[124]
A-44	$[Rb_2(H_2O)_3\{(H_2O)_{0.5}@Me_{10}Q[5]\}]\cdot PdCl_4$	2-D	[124]
A-45	$[Cs_2(H_2O)_2\{H_2O@Me_{10}Q[5]\}]\cdot PdCl_4$	0-D	[124]

A-46	$\{[Ag(H_2O)]_2(H_2O@Me_{10}Q[5])\}\cdot 2NO_3\cdot 2H_2O$	0-D	[125]
AE-1	$2\{Sr_2(H_2O)_8(HO)_1OMeQ[6]\}\cdot 3[CdCl_4]\cdot 2Cl\cdot 31H_2O$	1-D	[97]
AE-2	$\{Ba_2(H_2O)_8Cl[CdCl_4](HO)_1OMeQ[6]\}\cdot 2Cl\cdot H_3O\cdot 22H_2O$	1-D	[97]
AE-3	$2[Ca_2(H_2O)_8(NO_3@\textit{o}\text{-}TMeQ[6])]\cdot 2(CdCl_4)\cdot 4Cl\cdot 2H_3O\cdot 21H_2O$	1-D	[41]
AE-4	$2[Sr_2(H_2O)_9(NO_3@\textit{o}\text{-}TMeQ[6])]\cdot 2(CdCl_4)\cdot 2Cl\cdot 22H_2O$	1-D	[41]
AE-5	$\{(CaCl)(TMeQ[6])\}\cdot Cl\cdot 17.5H_2O$	0-D	[111]
AE-6	$\{(Sr_2Cl_2)[TMeQ[6]@H_2O]\}\cdot Cl_2\cdot 10H_2O$	1-D	[111]
AE-7	$\{Ca_2(H_2O)_4[(NO_3)@CyH_5Q[5]]\}_2(NO_3)_6\cdot 26H_2O$	0-D	[102]
AE-8	$\{Sr_2(H_2O)_3(NO_3)[(NO_3)@CyH_5Q[5]]\}(NO_3)_2\cdot 7H_2O$	1-D	[102]
AE-9	$\{Ba(H_2O)[(H_2O)_2@CyH_5Q[5]]\}(NO_3)_2\cdot 11H_2O$	1-D	[102]
AE-10	$\{Mg(H_2O)(Cl@CyP_5Q[5])\}\cdot 2[ZnCl_4]\ \cdot 3H_3O\cdot 15H_2O$	0-D	[103]
AE-11	$\{Ca_2(Cl@CyP_5Q[5])\}\cdot 2[ZnCl_4]\cdot H_3O\cdot 16H_2O$	0-D	[103]
AE-12	$2\{Sr_2(H_2O)_5(Cl@CyP_5Q[5])\}\cdot 2[ZnCl_4]\cdot [Zn(H_2O)Cl_3]\cdot Cl\cdot H_3O\cdot 8H_2O$	0-D	[103]
AE-13	$2\{Ba_2(H_2O)_3(Cl@CyP_5Q[5])\}\cdot 3[ZnCl_4]\cdot 23H_2O$	1-D	[103]
AE-14	$\{Mg(H_2O)6@CyP_6Q[6])\}\cdot 2[Zn(H_2O)Cl_3]\cdot 9H_2O$	0-D	[104]
AE-15	$\{Ca_2(H_2O)_8CyP_6Q[6]\}\cdot 2[ZnCl_4]\cdot 13(H_2O)$	1-D	[104]

AE-16	$\{Sr_2(H_2O)_{10}CyP_6Q[6]\}\cdot 2[ZnCl_4]\cdot 6(H_2O)$	1-D	[104]
AE-17	$\{Ba_2(H_2O)_{10}CyP_6Q[6]\}\cdot 2[ZnCl_4]\cdot 6(H_2O)$	1-D	[104]
AE-18	$\{Ca(H_2O)_4@HMe_6Q[6]\}[CdCl_4]\cdot 7H_2O$	1-D	[105]
AE-19	$\{Ba_2(H_2O)_8@HMe_6Q[6]\}[CdCl_4]\cdot 2Cl\cdot 12H_2O$	1-D	[105]
AE-20	$\{Ca_{1.5}(H_2O)_5(HO)_1Q[7]\}\cdot 2[CdCl_4]\cdot H_3O\cdot 35H_2O$	1-D	[106]
AE-21	$\{Sr_{1.5}(H_2O)_5(HO)_1Q[7]\}\cdot 2[CdCl_4]\cdot H_3O\cdot 35H_2O$	1-D	[106]
TM-1	$\{Cd_6Cl_{14}CyH_6Q[6]\}\cdot(H_3O)_2\cdot(H_2O)_2$	0-D	[108]
TM-2	$(TMeQ[6])\cdot(H_3O)_4^{4+}\cdot(CuCl_4)_2^{4-}\cdot 8H_2O$	0-D	[109]
TM-3	$[(TMeQ[6])(CuCl_2)_2(H_2O)_4]\cdot 10H_2O$	1-D	[109]
TM-4	$TMeQ[6]\cdot 14H_2O$	0-D	[109]
TM-5	$[Cu(H_2O)_4(C_4H_8O_2)@(CyH_6Q[6])]\cdot 2(NO_3)\cdot 4(H_2O)$	1-D	[110]
TM-6	$[Cu_2(H_2O)_6Cl_2(TMeQ[6])]\cdot 2Cl\cdot 15(H_2O)$	1-D	[110]
TM-7	$[Cu_2(H_2O)_9(TMeQ[6])]\cdot 2(SO_4)\cdot 16(H_2O)$	0-D	[110]
TM-8	$[(C_6H_{10}N_2)@(TMeQ[6])]\cdot CuCl_4\cdot 7(H_2O)$	0-D	[110]
TM-9	$[Cu(H_2O)_3\cdot CyP_5Q[5]]\cdot(ClO_4)_2$	1-D	[111]
TM-10	$[Zn_2(H_2O)_4\cdot(CyP_5Q[5])_2]\cdot(ClO_4)_4$	1-D	[111]

TM-11	$[Cu(H_2O)_2\cdot CyP_6Q[6]]\cdot(ClO_4)_2$	1-D	[111]
TM-12	$[Zn(H_2O)_2\cdot CyP_6Q[6]]\cdot(ClO_4)_2\cdot H_2O$	0-D	[111]
Ln-1-3	$\{LnCl_2(H_2O)_3CyH_5Q[5]\}\cdot NO_3\cdot 18.5H_2O$ Ln= La, Ce, Pr	1-D	[115]
Ln-4,5	$\{LnCl_2(H_2O)_2CyH_5Q[5]\}\cdot NO_3\cdot 14H_2O$ Ln=Nd, Sm	1-D	[115]
Ln-6	$\{Dy(H_2O)_2[Cl@CyH_5Q[5]]Dy(H_2O)_6\}\cdot 5Cl\cdot 20H_2O$	0-D	[115]
Ln-7,8	$\{LnCl(H_2O)[Cl@CyH_5Q[5]]Ln(H_2O)_6\}\cdot 4Cl\cdot 13H_2O$ Ln = Ho, Er	0-D	[115]
Ln-9-17	$[Ln(H_2O)_4](NO_3)_3\cdot CyH_6Q[6]\cdot nH_2O$, Ln = Y, Sm, Eu, Gd, Tb, Dy, Ho, Er, Yb	1-D	[116]
Ln-18	$\{Lu_2(H_2O)_{12}CyH_6Q[6]\}\cdot 4NO_3\cdot 2Cl\cdot 20H_2O$	1-D	[116]
Ln-19-21	$\{Ln_4(H_2O)_{16}[NO_3@CyH_6Q[6]]_2\}\cdot 10NO_3\cdot nH_2O$, Ln = La, Ce, Nd	0-D	[116]
Ln-22	$\{Pr(H_2O)_3Cl_2[NO_3@CyH_6Q[6]]\}\cdot 25H_2O$	0-D	[116]
Ln-23	$\{Pr(H_2O)_3Cl_2[NO_3@CyH_6Q[6]]\}\cdot 23H_2O$	0-D	[116]
Ln-24-27	$\{Ln_2(H_2O)_6(Cl@HMe_5Q[5])\}\cdot 2[CdCl_4]\cdot 2H_2O$ Ln = La, Ce, Pr, Nd	0-D	[117]
Ln-28-32	$\{HMe_6Q[6]\cdot[Ln(H_2O)_8]\}\cdot 3Cl\cdot nH_2O$ n=11-14, Ln = Tb, Dy, Ho, Er, Tm	0-D	[117]
Ln-33	$\{HMe_6Q[6]\cdot[Sm(H_2O)_8]\}\cdot 3Cl\cdot 10H_2O$	0-D	[117]
Ln-34-40	$\{o\text{-}TMeQ[6]\cdot[Ln(H_2O)_8]\}\cdot 2(NO_3)\cdot Cl\cdot 9H_2O$ Ln = Tb, Dy, Ho, Er, Tm, Yb, Lu	0-D	[118]
Ln-41	$La(H_2O)_4OMeQ[6]\}_2\cdot 2(CdCl_4)\cdot[CdCl_2(H_2O)_4]\cdot 16H_2O$	1-D	[119]

Ln-42	$\{(NO_3)_2@OMeQ[6]\cdot Ce_2(H_2O)_{10}\}\cdot 2(CdCl_4)\cdot 10H_2O$	0-D	[119]
Ln-43,44	$\{Cl@OMeQ[6]\cdot Ln_2(H_2O)_9\}\cdot 2(CdCl_4)\cdot 3Cl^-\cdot nH_2O$ Ln = Pr, Eu	0-D	[119]
Ln-45	$\{OMeQ[6]\cdot Nd_2(H_2O)_{12}\}\cdot 2(CdCl_4)\cdot 2Cl^-\cdot 4H_2O$	0-D	[119]
Ln-46	$OMeQ[6]\cdot Sm(H_2O)_8\cdot (CdCl_4)\cdot NO_3^-\cdot 3H_2O$	0-D	[119]
Ln-47-49	$OMeQ[6]\cdot Ln(H_2O)_8\cdot (CdCl_4)\cdot Cl^-\cdot nH_2O$ Ln= Gd, Dy, Ho	0-D	[119]
Ln-50	$\{(C_6H_6O_2)@OMeQ[6]\cdot Ho_2(H_2O)_{10}\}\cdot 2(CdCl_4)\cdot (C_6H_6O_2)\cdot 4Cl^-\cdot 4(H_3O)^+\cdot 8H_2O$	0-D	[119]
Ln-51-53	$\{Ln(H_2O)_6\cdot CyP_6Q[6]\}\cdot 2[ZnCl_4]\cdot Cl\cdot 2(H_3O)\cdot n(H_2O)$ Ln = La, Ce, Sm	0-D	[120]
Ln-54-59	$\{Ln(H_2O)_5\cdot CyP_6Q[6]\}\cdot 2[ZnCl_4]\cdot (H_3O)\cdot n(H_2O)$ Ln = Pr, Nd, Eu, Gd, Tb, Dy	0-D	[120]
Ln-60	$CyP_6Q[6]\cdot [Ho(H_2O)_8]\cdot [ZnCl_4]\cdot [Zn(H_2O)Cl_3]\cdot 15(H_2O)$	0-D	[120]
Ln-61-69	$\{t(HO)_2OMeQ[6]\cdot [Ln(H_2O)_8]\}\cdot x(NO_3)\cdot yCl\cdot zH_2O$ Ln = Eu, Gd, Tb, Dy, Ho, Er, Tm, Yb, Lu	0-D	[121]
Ln-70-72	$\{Ln(H_2O)_5(NO_3)(o\text{-}TMeQ[6])\}\cdot (NO_3)_2\cdot 6H_2O$ Ln = Nd, Sm, Eu	0-D	[122]
Ln-73-80	$\{Ln(H_2O)_6(o\text{-}TMeQ[6])\}\cdot 2(NO3)\cdot Cl\cdot nH_2O$ Ln= Gd, Tb, Dy, Ho, Er, Tm, Yb, Lu	0-D	[122]
Ln-81-84	$\{Ln(H_2O)_6CyH_6Q[6]\}\cdot 2(CdCl_4)\cdot H_3O\cdot nH_2O$ Ln = La, Ce, Pr, Nd	1-D	[123]
Ln-85	$\{Sm(H_2O)_5CyH_6Q[6]\}\cdot 2(CdCl_4)\cdot H_3O\cdot 10H_2O$	1-D	[123]
Ln-86-88	$\{Ln(H_2O)_5(NO_3)@CyH_6Q[6]\}\cdot 2(CdCl_4)\cdot 2H_3O\cdot nH_2O$ Ln = Gd, Tb, Dy	1-D	[123]

Table 3 The coordination conditions and results of substituted Q[*n*]s with lanthanide ions.*

Ligand	La	Ce	Pr	Nd	Sm	Eu	Gd	Tb	Dy	Ho	Er	Tm	Yb	Lu	Ref.
$CyH_5Q[5]$ in water	√	√	√	√	√	—	—	—	√	√	√	—	—	—	[115]
$CyH_6Q[6]$ in water	√	√	√	√	√	√	√	√	√	√	√	—	√	√	[116]
$HMe_5Q[5]$ in $[CdCl_4]^{2-}$	√	√	√	√	×	×	×	×	×	×	×	×	×	×	[117]
$HMe_6Q[6]$ in $[CdCl_4]^{2-}$	×	×	×	×	×	×	√	√	√	√	√	√	√	√	[117]
$HMe_6Q[6]$ in water	×	×	×	×	√	√	√	√	√	√	√	√	√	√	[117]
o-TMeQ[6] in neutral sol.	×	×	×	×	×	×	×	√	√	√	√	√	√	√	[118]
OMeQ[6] in $[CdCl_4]^{2-}$	√	√	√	√	√	√	√	—	√	√	×	×	×	×	[119]
$CyP_6Q[6]$ in $[ZnCl_4]^{2-}$	√	√	√	√	√	√	√	√	√	√	√	○	○	○	[120]
$(HO)_2OMeQ[6]$ in water	×	×	×	×	×	√	√	√	√	√	√	√	√	√	[121]
o-TMeQ[6] in $Cd(NO_3)_2$	×	×	×	√	√	√	√	√	√	√	√	√	√	√	[122]
$CyH_6Q[6]$ in $[CdCl_4]^{2-}$	√	√	√	√	√	√	—	√	√	○	×	○	○	×	[123]

* Promethium is not discussed and contained because it is a radioactive element

× No crystals were obtained, √ Obtained crystals contain lanthanide ions, — no information, ○ The obtained crystals without lanthanide ions.

Synopsis

View Article Online
DOI: 10.1039/D0QI00529K

Supramolecular Chemistry of Substituted Cucurbit[*n*]urils

Rui-Lian Lin,[a] *Jing-Xin Liu*[a,]* *Kai Chen*[b,]* *and Carl Redshaw*[c]

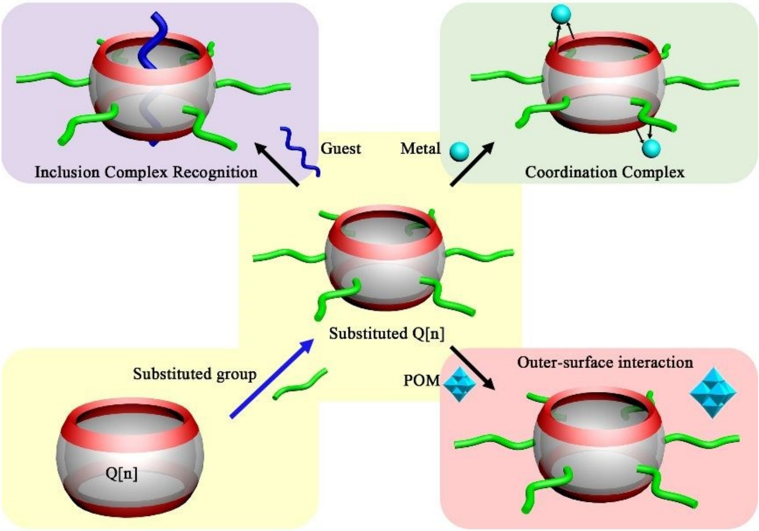

This review covers important advances in the field of substituted cucurbit[*n*]urils.